Botanical Journal of the Linnean Society, 2017, **183**, 474–499. With 8 figures.

Morphological convergence in the recently diversified *Silene gigantea* complex (Caryophyllaceae) in the Balkan Peninsula and south-western Turkey, with the description of a new subspecies

PIERRE-EMMANUEL DU PASQUIER[1,2], DANIEL JEANMONOD[1,2] and YAMAMA NACIRI[1,2]*

[1]*Unité de phylogénie et génétique moléculaires, Conservatoire et Jardin botaniques, CH-1292 Chambésy, Geneva, Switzerland*
[2]*Plant Systematics and Biodiversity Laboratory, Department of Plant Biology, Science Faculty, University of Geneva, CH-1292 Chambésy, Geneva, Switzerland*

Received 1 April 2016; revised 24 October 2016; accepted for publication 23 November 2016

The *Silene gigantea* complex is characterized by a high degree of morphological variability that resulted in the description of three subspecies across its distribution range from the Balkan Peninsula to South-west Asia and Cyprus. In this work, we used nuclear and plastid markers in Bayesian phylogeographic analyses to investigate the taxonomy and the evolutionary history of *S. gigantea*. The results from plastid DNA partly support the existing taxonomic assessments since *S. gigantea* subsp. *rhodopea* is monophyletic, whereas *S. gigantea* subspp. *gigantea* and *hellenica* are clearly polyphyletic. This pattern suggests that a strong morphological convergence is associated with chasmophytic conditions. The results also suggest that the populations from the Epirus region (north-western Greece) did not arise from hybridization as previously claimed, but correspond to a new evolutionary lineage that is consequently described and named *S. gigantea* subsp. *epirota*. An identification key to the four subspecies is also given. Our phylogeographic study further highlights a genetic continuity across populations from the central and eastern Greek mainland to Chios and Turkey, all of them sharing the same plastid DNA haplotype and belonging to the same nuclear cluster. In addition, at least two separate colonization events are suggested for Crete. The Bayesian phylogeographic reconstruction clearly points to a post-Messinian diversification across the Aegean area. Considering the low seed dispersal ability of *S. gigantea*, a continuum of ancestral populations between islands and the mainland is assumed to have occurred during the last glaciations and to have played a key role in colonization processes.

ADDITIONAL KEYWORDS: Aegean area – Bayesian analyses – internal transcribed spacer – phylogeography – plastid DNA markers – population genetics – *Silene gigantea* subsp. *epirota* – spatial analyses.

INTRODUCTION

In the eastern part of the Mediterranean Basin, the Balkan Peninsula and South-west Asia are considered as centres of diversity and endemism for plants and animals (Zohary, 1973; Polunin, 1980; Strid & Tan, 1997; Kryštufek & Reed, 2004; Nieto Feliner, 2014). For most Aegean taxa, the current biogeographic patterns were shaped by complex geological events that occurred during the Miocene and by more recent eustatic variations, climatic changes, retreats in post-glacial refugia and human activities since the Pliocene (Polunin, 1980; Kryštufek & Reed, 2004; Tzedakis, 2004; Triantis and Mylonas, 2009). In recent decades, numerous studies have explored the biogeographic patterns of species or groups of species, especially for animals, in the island-mainland system of the Aegean area (see Poulakakis *et al.*, 2015 for a review) or in the Levantine Basin.

Silene L. (Caryophyllaceae) is one of the most diverse genera in the eastern part of the Mediterranean and the Middle East (Zohary, 1973). One of its diversity

*Corresponding author. E-mail: yamama.naciri@ville-ge.ch

centres is in Turkey, Greece and Cyprus with endemic rates as high as 45% (Coode & Cullen, 1967; Davis, 1971; Yıldız, Mınarecı & Çırpıcı, 2009; Yıldız & Çırpıcı, 2013), 38% (Greuter, 1997; Trigas, Iatrou & Karetsos, 2007) and 15% (Meikle, 1977; Hand, Hadjikyriakou & Christodoulou, 2011), respectively. *Silene gigantea* (L.) L. has been recently shown to form a strongly supported clade, sister to section *Italicae* (Rohrb.) Schischk. (Naciri *et al.*, 2017). *Silene gigantea* is a morphologically variable species with $2n = 24$ chromosomes (Ghazanfar, 1983; Strid & Andersson, 1985; Yıldız *et al.*, 2008) that grows preferentially on calcareous substrates from 20 to 1200 m elevation. As for other *Silene* spp., seed dispersal capacity is limited to the vicinity of the mother plant (Montesinos, García-Fayos & Mateu, 2006; P. Authier, personal communication). On islands (Ionian, Aegean, Crete, Karpathos and Cyprus), *S. gigantea* grows as a chasmophyte and has a characteristic morphology that consists of a condensed inflorescence in a verticillaster with many flowers and glandular or eglandular long hairs (or both) on the calyx (Du Pasquier, Naciri & Jeanmonod, 2015). Such populations correspond to the type subspecies. In contrast, populations from the northern Balkan Peninsula have a lax inflorescence with few flowers and exclusively small glands on the calyx. The latter populations are referred to *S. gigantea* subsp. *rhodopea* (Janka) Greuter. Finally, populations from central and eastern Greece and Turkey, corresponding to *S. gigantea* subsp. *hellenica* Greuter, display an intermediate morphology with glandular long hairs on the calyx (Greuter, 1995; Du Pasquier *et al.*, 2015).

Du Pasquier *et al.* (2015) analysed the distribution and morphology of the biennial (or monocarpic perennial) and gynodioecious *S. gigantea* complex using specimens from the Balkan Peninsula (Greece, Bulgaria, Macedonia, Albania and Serbia), south-western Turkey and Cyprus. The three subspecies, previously recognized in Greece by Greuter (1995, 1997), were supported morphologically using a substantial number of individuals from the whole distribution of the species. The main result was the assignment of all Turkish populations to *S. gigantea* subsp. *hellenica*, which was initially described from the Peloponnese and central and eastern Greece only (Greuter, 1995, 1997). The occurrence of *S. gigantea* subsp. *rhodopea* in Turkey, reported by many authors (Coode & Cullen, 1967; Yıldız, 2006; Yıldız & Çırpıcı, 2013), was invalidated, whereas the presence of *S. gigantea* subsp. *gigantea* was confirmed on Cyprus. Furthermore, the populations from Epirus (north-western Greece), known to display intermediate morphological features (Greuter, 1995), were suggested to result from a colonization of the mainland by Ionian populations of *S. gigantea* subsp. *gigantea* (Du Pasquier *et al.*, 2015) and not from hybridization between *S. gigantea* subspp. *gigantea* and *rhodopea* as suggested by Greuter (1995, 1997).

In the present study, we explored the genetic structure of the *S. gigantea* complex across its distribution using a population genetic approach as described in Avise (2000) and Posada & Crandall (2001). We used two plastid markers (*trnH-psbA* and *trnS-trnG*) and one nuclear marker [the nuclear ribosomal internal transcribed spacer (ITS)], as these markers already provided a good resolution for phylogeographic analyses and taxonomic delimitations of *Silene* spp. (Frajman & Oxelman, 2007; Frajman, Eggens & Oxelman, 2009; Naciri, Cavat & Jeanmonod, 2010; Rautenberg *et al.*, 2010; Greenberg & Donoghue, 2011; Aydin *et al.*, 2014; Leuzinger *et al.*, 2015; Naciri *et al.*, 2017). Moreover, we performed a taxonomic delimitation and phylogeographic analyses using geolocated data in a Bayesian framework. More precisely, the objectives are (1) to investigate the evolutionary history of the *S. gigantea* complex in a phylogeographic context; (2) to confirm or refute the taxonomic assessments of Greuter (1995, 1997) and Du Pasquier *et al.* (2015) and, more specifically, to challenge previous hypotheses concerning the populations from the Epirus region.

MATERIAL AND METHODS

Plant material

Two hundred and forty-seven individuals of *S. gigantea* from 62 populations (one to eight individuals per population, see Table 1) were analysed. Among these populations, 37 were collected in Greece during May–June 2011 and 2012 and leaves of five individuals per population were dried in silica gel in the field. The remaining individuals were gathered from herbarium specimens in G, MAIC, MUFE, P and Z and the personal herbarium of J. Zaffran (Kolympari, Crete). This sampling covers the whole distribution of *S. gigantea*. Specimens analysed morphologically by Du Pasquier *et al.* (2015) are highlighted in Table 1.

Distribution map

The distribution map was drawn using the Quantum GIS software Version 1.8.0 (http://qgis.org/fr/site/). The phytogeographical subdivisions of Greece, Turkey and Cyprus (see Appendix 1) are based on Rechinger's works (Rechinger, 1950; Rechinger & Rechinger-Moser, 1951), *Flora Hellenica* (Strid & Tan, 1997), *Flora of Turkey* (Coode & Cullen, 1967; Kürschner, Raus & Venter, 1995) and *Flora of Cyprus* (Meikle, 1977).

Table 1. Analysed populations with their characterisation (collector name, collector number, population name, country, region, coordinates in decimal degrees, sampling size), cpDNA haplotypes, Geneland groups, gene diversity (h_s) and allelic richness (R_s) for the nuclear marker ITS. Asterisks indicate the populations analysed morphologically in Du Pasquier et al. (2015). The Greek phytogeographic regions are given with the following code: EAe East Aegean area, IoI Ionian Islands, CK Crete Karpathos, NC North Central, NE North Eastern, NPi Northern Pinde, Pe Peloponnese, StE Sterea Ellas, SPi Southern Pinde. For Turkey and Cyprus, see Kürschner et al. (1995) and Meikle (1977), respectively.

Collectors, collectors number (herbarium)	Population	Country	Region	Latitude	Longitude	Sample size	cpDNA haplotypes	ITS		Geneland groups
								h_S	R_S	
S. gigantea subsp. gigantea										
Du Pasquier, P.-E., C. Christe & M. Esmerode, 121 (G)	S071*	Greece: IoI	Lefkás	20.68° N	38.83° E	3 2	A26B44 A26	0.600	1.533	5
Du Pasquier, P.-E. & A. Cusin, 222 (G)	S158	Greece: IoI	Lefkás	20.55° N	38.59° E	1	A26B44	-	2.000	5
Du Pasquier, P.-E. & A. Schlüssel, 154 (G)	S104*	Greece: EAe	Rhodos Island	27.92° N	36.27° E	5	A26B47	0.875	1.867	4
Du Pasquier, P.-E. & A. Schlüssel, 155 (G)	S105*	Greece: EAe	Samos Island	26.85° N	37.80° E	4 1	A26B47 A26	0.650	1.689	4
Du Pasquier, P.-E. & A. Schlüssel, 157 (G)	S107*	Greece: Eae	Samos Island	26.65° N	37.72° E	5	A26B47	0.950	1.889	4
Jeanmonod, Daniel, 8138 (G)	DJ8138	Greece: CK	Karpathos	27.14° N	35.56° E	5	A76B46	-	-	-
Jeanmonod, Daniel, 8139 (G)	DJ8139	Greece: CK	Karpathos	27.17° N	35.58° E	1	A76B46	-	-	-
Jeanmonod, Daniel, 8140 (G)	DJ8140	Greece: CK	Karpathos	27.13° N	35.59° E	5	A75B46	-	-	-
Jeanmonod, Daniel, 8141 (G)	DJ8141	Greece: CK	Karpathos	27.13° N	35.59° E	1	A75B46	-	-	-
Du Pasquier, P.-E. & A. Cusin, 216 (G)	S152	Greece: CK	Crete	24.39° N	35.21° E	6	A49B47	0.000	1.000	2
Du Pasquier, P.-E. & A. Cusin, 217 (G)	S153	Greece: CK	Crete	24.40° N	35.22° E	5	A49B47	0.000	1.000	2
Du Pasquier, P.-E. & A. Cusin, 221 (G)	S157	Greece: CK	Crete	26.05° N	35.02° E	5	A49B47	0.500	1.500	2
Greuter, W., 4091 (G)	SH032	Greece: CK	Crete	25.65° N	35.06° E	1	A49	-	-	2
	SH043					1	A49	-	-	2
Greuter, W., 4098S (G)	SH041*	Greece: CK	Crete	25.65° N	35.17° E	1	A49B47	-	1.000	2
Unkown, s.n. (MAIC)	SH127	Greece: CK	Crete	24.45° N	35.18° E	1	A49B44	-	1.000	2
Zaffran, J., 920 (herb. ZAFFRAN)	SH99	Greece: CK	Crete	23.89° N	35.33° E	1	-	-	1.000	2

Table 1. Continued

Collectors, collectors number (herbarium)	Population	Country	Region	Latitude	Longitude	Sample size	cpDNA haplotypes	ITS		Geneland groups
								h_S	R_S	
S. gigantea* subsp. *hellenica										
Du Pasquier, P.-E. & A. Schlüssel, 66 (G)	S016*	Greece: Pe	Laconia	22.38° N	37.06° E	5	A24B44	0.000	1.000	2
Du Pasquier, P.-E. & A. Schlüssel, 67 (G)	S017	Greece: Pe	Laconia	22.38° N	37.06° E	5	A24B44	0.000	1.000	2
Du Pasquier, P.-E. & A. Schlüssel, 69 (G)	S019*	Greece: Pe	Laconia	22.39° N	37.04° E	5 1	A24B44 B44	0.650	1.644	2
Du Pasquier, P.-E. & A. Schlüssel, 71 (G)	S021	Greece: Pe	Laconia	22.39° N	37.05° E	5	A24B44	0.700	1.733	2
Du Pasquier, P.-E. & A. Schlüssel, 73 (G)	S023	Greece: Pe	Laconia	22.33° N	37.09° E	5	A24B44	0.200	1.200	2
Du Pasquier, P.-E. & A. Schlüssel, 75 (G)	S025	Greece: Pe	Laconia	22.29° N	37.08° E	5	A24B44	0.350	1.356	2
Du Pasquier, P.-E. & A. Schlüssel, 76 (G)	S026	Greece: Pe	Messenia	22.28° N	37.07° E	5	A24B44	0.500	1.533	2
Du Pasquier, P.-E. & A. Schlüssel, 78 (G)	S028*	Greece: Pe	Messenia	22.17° N	37.09° E	5	A24B44	0.583	1.607	2
Du Pasquier, P.-E. & A. Schlüssel, 79 (G)	S029*	Greece: Pe	Messenia	22.23° N	37.07° E	5	A24B44	0.500	1.533	2
Du Pasquier, P.-E. & A. Schlüssel, 80 (G)	S030*	Greece: Pe	Messenia	22.22° N	37.08° E	5	A25B44	0.700	1.689	2
Du Pasquier, P.-E. & L. Fazan, 170 (G)	S120*	Greece: Pe	Corinthia	22.23° N	38.13° E	5	A26B46	0.333	1.333	3
Du Pasquier, P.-E., 95 (G)	S045*	Greece: StE	Corinthia	22.56° N	37.88° E	2 3	A26B44 A26B46	0.500	1.511	3
Du Pasquier, P.-E., C. Christe & M. Esmerode, 107 (G)	S057*	Greece: StE	Beotia	22.60° N	38.48° E	5	A26B46	0.583	1.607	3
Du Pasquier, P.-E., C. Christe & M. Esmerode, 110 (G)	S060*	Greece: StE	Beotia	22.56° N	38.49° E	5	A26B46	0.550	1.533	3
Du Pasquier, P.-E., C. Christe & M. Esmerode, 118 (G)	S068	Greece: StE	Evrytania	21.73° N	38.82° E	5	A26B44	0.583	1.536	2

Table 1. Continued

Collectors, collectors number (herbarium)	Population	Country	Region	Latitude	Longitude	Sample size	cpDNA haplotypes	ITS		Geneland groups
								h_S	R_S	
Du Pasquier, P.-E., 105 (G)	S055*	Greece: Wae	Euboea	23.32° N	38.79° E	5	A26B46	0.750	1.778	3
Rechinger, K. H., 16544 (G)	SH013	Greece: Wae	Euboea	23.35° N	38.80° E	1	A26B46	-	-	3
Du Pasquier, P.-E. & A. Schlüssel, 159 (G)	S109*	Greece: EAe	Chios	26.00° N	38.38° E	5	A26B46	0.950	1.956	4
Du Pasquier, P.-E. & A. Schlüssel, 161 (G)	S111*	Greece: EAe	Chios	26.04° N	38.57° E	5	A26B46	0.875	1.867	4
Hubert-Morath, A., 2157 (G)	SH003*	Turkey: 2.2	İzmir	28.36° N	37.44° E	1	A26B46	-	-	3
Hubert-Morath, A., 12287 (G)	SH001	Turkey: 2.1	Muğla	28.36° N	37.21° E	1	A26B46	0.750	1.833	3
Hubert-Morath, A., 5842 (G)	SH002	Turkey: 2.1	Muğla	29.54° N	36.99° E	1	A26B46	-	2.000	3
Çirpici, A. & K. Yildiz, 102-3 (MUFE)	SH038	Turkey: 2.1	Denizli	28.85° N	37.78° E	1	A26B46	-	1.000	3
Çirpici, A. & K. Yildiz, 113 (MUFE)	SH039*	Turkey: 3.1	Antalya	30.43° N	36.75° E	1	A26B46	-	1.000	3
Yildiz, K. & M. Y. Dadandi, 36-1 (MUFE)	SH040	Turkey: 3.1	Antalya	29.94° N	36.56° E	1	A49	-	2.000	3
Du Pasquier, P.-E., C. Christe & M. Esmerode, 120 (G)	S070*	Greece: SPi	Aetolia-Acarnania	21.61° N	38.64° E	5	A26B44	0.000	1.000	2
S. gigantea* subsp. *rhodopea										
Du Pasquier, P.-E., C. Christe & M. Esmerode, 129 (G)	S079	Greece: NC	Florina	21.77° N	40.68° E	4 1	A51B44 A51	0.000	1.000	2
Du Pasquier, P.-E., C. Christe & M. Esmerode, 135 (G)	S085	Greece: NC	Emathia	22.22° N	40.45° E	1 4	A48B44 A51B44	0.000	1.000	2
Du Pasquier, P.-E., C. Christe & M. Esmerode, 136 (G)	S086	Greece: NC	Emathia	22.20° N	40.40° E	5	A51B44	0.000	1.000	2

Table 1. Continued

Collectors, collectors number (herbarium)	Population	Country	Region	Latitude	Longitude	Sample size	cpDNA haplotypes	ITS		Geneland groups
								h_S	R_S	
Du Pasquier, P.-E., C. Christe & M. Esmerode, 137 (G)	S087*	Greece: NC	Pieria	22.27° N	40.34° E	5	A51B44	0.400	1.356	2
Du Pasquier, P.-E., C. Christe & M. Esmerode, 140 (G)	S090*	Greece: NC	Larissa	22.18° N	39.91° E	5	A51B44	0.667	1.643	2
Du Pasquier, P.-E. & L. Fazan, 197 (G)	S136*	Greece: NC	Florina	22.16° N	41.08° E	5	A48B44	0.375	1.378	2
Du Pasquier, P.-E. & L. Fazan, 201 (G)	S140	Greece: NE	Serres	23.54° N	41.16° E	7 1	A46B44 A46	0.000	1.000	2
Du Pasquier, P.-E. & L. Fazan, 206 (G)	S143*	Greece: NE	Drama	24.13° N	41.16° E	5	A48B58	0.825	1.822	2
Du Pasquier, P.-E. & L. Fazan, 207 (G)	S144*	Greece: NE	Xanthi	24.68° N	41.20° E	1 4	A51B44 A52B44	0.500	1.511	2
Behr, s.n. (G)	SH004*	Macedonia	Vodno Mountain	21.39° N	41.96° E	1	A46B44	-	1.000	2
Strid, A. , 46798 (G)	SH009*	Greece: NC	Pella	21.86° N	40.75° E	1	A51B44	-	1.000	2
Rechinger, K. H., 3283b (G)	SH010 SH011	Greece: NC	Edessa	22.05° N	40.80° E	1 1	A48B44 A51B44	1.000 -	1.667 -	2
Hartvig, P. & S. G. Christiansen, 8500 (G)	SH014*	Greece: NC	Grevena	21.58° N	40.18° E	1	A51B44	-	1.000	2
Rechinger, K. H. & F. Rechinger, 5990 (G)	SH020	Greece: NE	Alexandroupolis	25.73° N	40.85° E	1	A51B44	-	-	2
Rechinger, K. H. & F. Rechinger, 6034 (G)	SH021*	Greece: NE	Alexandroupolis	25.88° N	40.90° E	1	B44	-	-	2
Burdet, H. M. & A. Charpin, 10203 (G)	SH015*	Greece: NE	Serres	23.53° N	41.08° E	1	A46B44	-	2.000	2
Stříbrny, V., s.n. (G)	SH025*	Bulgaria	Pazardzhik	24.33° N	42.20° E	1	A46	-	-	2
Stříbrny, V., s.n. (G)	SH026	Bulgaria	Tekir	24.68° N	41.45° E	1	A46B44	-	-	2
Epirus groups										
Du Pasquier, P.-E., C. Christe & M. Esmerode, 123 (G)	S073*	Greece: SPi	Arta	20.84° N	39.28° E	4 1	A26B44 A26	0.000	1.000	1
Du Pasquier, P.-E., C. Christe & M. Esmerode, 148 (G)	S098*	Greece: SPi	Ioannina	20.92° N	39.68° E	5 2	A26B44 A26	0.400	1.356	1

Table 1. Continued

Collectors, collectors number (herbarium)	Population	Country	Region	Latitude	Longitude	Sample size	cpDNA haplotypes	ITS		Geneland groups
								h_s	R_s	
Du Pasquier, P.-E., C. Christe & M. Esmerode, 149 (G)	S099	Greece: SPi	Ioannina	20.48° N	39.58° E	5	A26B44	0.000	1.000	1
Du Pasquier, P.-E., C. Christe & M. Esmerode, 151 (G)	S101*	Greece: SPi	Thesprotia	20.48° N	39.28° E	5	A26B44	0.550	1.511	1
Jeanmonod, D., 8070 (G)	DJ8070	Greece: NPi	Zagoria	20.69° N	39.90° E	2	A26B44	0.000	1.000	1
Du Pasquier, P.-E., C. Christe & M. Esmerode, 147 (G)	S097*	Greece: NPi	Ioannina	21.05° N	37.40° E	5 1	A26B44 A26	0.000	1.000	1

DNA EXTRACTION AND AMPLIFICATION

Total DNA was extracted from field-collected and herbarium specimens using the Plant DNEasy kit (Qiagen) following the manufacturer's instructions with a 30-min incubation phase for cell lysis. Two 50 µL elution solutions were obtained for each sample and stored in a –20 °C freezer. The second elution was used for further analyses. Polymerase chain reaction (PCR) amplifications were performed for two plastid spacers, *trnH-psbA* (HA) and *trnS-trnG* (SG) using different sets of primers, and for nuclear ITS (Appendix 2). Amplifications were usually difficult to obtain from herbarium samples and nested-PCR had to be used (see details in Appendix 2). Additional information about PCR and sequence reactions is given in Appendix 2. DNA sequences were obtained from purified DNA on NucleoFast© plates (Macherey-Nagel) using either the BigDye Sequencing kit (Applied Biosystems) and run on an ABI PRISM 377 DNA automated sequencer (PE Biosystems) as described by Naciri *et al.* (2010), or using the GenomeLab Quick Start kit and run on a CEQ 8800 automated sequencer (Beckman Coulter). All sequences are available on GenBank (Appendix 3).

SEQUENCE ASSEMBLY

Sequences were assembled and corrected using Sequencher software version 5.1 (Gene Codes Corporation) and aligned manually in BioEdit version 7.1.3.0 (Hall, 1999). Indels (gaps) and inversions, which are known to have high informative content at the intraspecific level in *Silene* (Ingvarsson, Ribstein & Taylor, 2003; Naciri *et al.*, 2010; Leuzinger *et al.*, 2015), were taken into account and coded following Barriel's rules (1984) for the median-joining network or following the 'simple gap coding' principle of Simmons & Ochoterena (2000) for the phylogenetic analyses (see below). Plastid haplotypes were identified and named using BioEdit alignments, whereas the software Phase (Stephens, Smith & Donnelly, 2001) was used to help defining phasing and ribotypes in heterogeneous ITS sequences as performed in Leuzinger *et al.* (2015). Haplotype and ribotype names were coded following Naciri *et al.* (2010) and Leuzinger *et al.* (2015).

GENETIC CLUSTERING

We inferred the number of genetic groups for ITS sequences using Geneland package version 4.0.3. (Guillot *et al.*, 2005a; Guillot, Mortier & Estoup 2005b; Guillot, 2008) in R version 2.15.2 (R Development Core Team, 2012). This program uses a Bayesian clustering method (Markov chain Monte Carlo) and considers georeferenced individuals. Ribotypes as recovered using the program Phase were reported in the input data set. Two different simulations, each with ten independent runs, were performed with the following parameters: 1 000 000 iterations with 100 thinning intervals and the uncorrelated allele frequency model. Following the authors' advice, the maximum group number (K_{max}) used in the first simulation corresponded to the number of analysed populations, whereas in the second simulation, K_{max} was fixed as the highest group number obtained in the first simulation. Not all populations could be sequenced for ITS and K_{max} was therefore fixed to 55 for the first run. The posterior probability maps were drawn with 100 × 100 pixels and a burn-in of 50 iterations.

GENETIC DIVERSITY

The genetic diversity and differentiation of *S. gigantea* were computed on plastid DNA and ITS with two approaches for the delimitation of population groups, that is the genetic clustering resulting from Geneland analyses and the taxonomic clustering of Du Pasquier *et al.* (2015), who recognized three subspecies in the complex (*S. gigantea* subspp. *gigantea*, *hellenica* and *rhodopea*) and one additional group. This additional group (the 'Epirus group') comprises populations from north-western Greece that display intermediate morphological features. This group is either assumed to result from an ancient colonization of the mainland by Ionian populations of *S. gigantea* subsp. *gigantea* (Du Pasquier *et al.*, 2015) or to be of hybrid origin between *S. gigantea* subspp. *gigantea* and *rhodopea* (Greuter, 1995, 1997).

Complete linkage disequilibrium between pairs of plastid loci was confirmed using Fisher's exact test in Arlequin version 3.5.1.2 (Excoffier & Lischer, 2010). Estimates of the following molecular indices were obtained using Fstat version 2.9.3.2 (Goudet, 1995) for plastid DNA and ITS: unbiased gene diversity (h_T), average intra-population diversity (h_S) (Nei & Chesser, 1983), population allelic richness (R_S) and overall allelic richness (R_T) using the rarefaction technique implemented in Fstat. Arlequin was used to estimate nucleotide diversities π (Tajima, 1983; Nei, 1987) with their standard deviation for each morphological group and for Geneland clusters. Tajima's D (Tajima, 1983) and Fu's F_S (Fu, 1997) statistics, used to test for neutral evolution but also known to be sensible to population dynamics such as bottlenecks or population expansions, were computed from the plastid markers using 20 000 permutations in Arlequin. Analyses of molecular variance (AMOVA) for each of the two clustering (morphology and Geneland) were conducted to estimate the genetic differentiation among populations (Φ_{ST}) and groups of populations (Φ_{CT}) using pairwise

differences as genetic distance between plastid DNA sequences to take into account indels and Tamura & Nei's distance for ITS.

Plastid haplotype network

Networks for plastid DNA were drawn using the median joining method (Bandelt, Forster & Röhl, 1999) implemented in Network 4.6.1.2 (Fluxus Technology) on HA and SG concatenation. A first haplotype network was built with all mutations weighted equally, including indels and inversions (network not shown). To reduce the impact of homoplasy, a second network was then built with mutations/indels/inversions inversely weighted by the number of times they appeared in the first network as suggested by Bandelt *et al.* (1999).

Bayesian analyses

Bayesian analyses were performed with BEAST version 1.8.2 (Heled & Drummond, 2010) using the TN93 + gamma substitution model and the coalescent extended Bayesian Skyline plot approach on the concatenated plastid markers HA-SG and on ITS. For the plastid markers, an uncorrelated lognormal relaxed clock was used with a mutation rate (ucld.mean: normal; 0.0.025; 0.0008) ranging from 1×10^{-9} to 5×10^{-9} per site per year [estimation from Taylor *et al.*, 2007, for *Silene vulgaris* (Moench) Garcke]. This estimation falls well within the range found for angiosperms (Wolfe & Sharp, 1988). We used a lognormal model (10; 5) for root height (TreeModel.rootheight) and a lognormal model (3; 3) for the demographic population mean (Demo.pop.mean). We ran four independent MCMC for 50 000 000 generations with tree sampling fixed every 5000 generations. Tracer version 1.6.0 was used to check for ESS values and LogCombiner to combine the trees from different runs. We generated a maximum clade credibility (MCC) tree in TreeAnnotator with a burn-in fixed at 10%. To model phylogeography of *S. gigantea*, we generated a second tree with BEAST using the previous parameters, taking into account the geographical position of sampled individuals as an additional trait. As each population was represented by more than one sample, the jitter option was activated. The final MCC tree was analysed with Spread version 1.0.6 (Spatial Phylogenetic Reconstruction of Evolutionary Dynamics; Bielejec *et al.*, 2011), which allows the visualization of ancestral areas in Google Earth (https://www.google.ch/intl/fr/earth/). For ITS, we obtained a tree using *BEAST (Heled & Drummond, 2010) and the GTR + gamma substitution model. We used the Yule process with piecewise linear and constant root, a lognormal (3, 3) prior for the species population mean (Species.pop.mean) and a lognormal (0, 1) for the species Yule birth death rate (species.yule.birthdeathRate). Two independent runs of 2000 trees each were obtained from 10 000 000 MCMC. An MCC tree was generated as for plastid DNA markers (see above).

RESULTS

Success of DNA amplification

PCR was attempted on 285 individuals, 244 of which were sequenced for at least one marker (see details in Appendix 4). Approximately 21% of herbarium samples were successfully sequenced for the three loci compared to 82% for silica-dried material. The amplification success depended greatly on specimen age and sequence length and was most probably influenced by the unknown drying conditions of the herbarium specimens. A single individual from Cyprus (herbarium specimen dating from 1883) could be sequenced, but only for the two plastid spacers. The haplotype for HA differed from all other ones by seven mutations. Since this haplotype was not found in any other individual and as it presented a nonsynonymous mutation in the *psbA* coding region, besides being amplified from quite an old herbarium specimen for which DNA damage could also be suspected (Staats *et al.*, 2011), we assumed that it corresponds to a paralogous sequence (NuPt; Arthofer *et al.*, 2010; Naciri & Manen, 2010). We therefore discarded this individual from all analyses, although it meant that no individual from Cyprus could be included.

ITS diversity and overall differentiation

The trimmed and aligned ITS region was 760 bp length and included the complete ITS1, 5.8S, ITS2 and 82 bp of the 26S ribosomal RNA. Two hundred and four individuals from 55 populations were sequenced (one to eight individuals per population). The available specimens from Cyprus and Karpathos could not be sequenced for ITS, despite several attempts. The ITS alignment contained 32 polymorphic sites and no indels. The Phase software allowed for the identification of ITS variants. Fifty-six ribotypes were found (named I107–I187) from the 64 different genotypes that were used in Geneland.

ITS diversity estimates are shown in Tables 1 and 2. Considering the species as a whole, the overall ITS ribotype diversity was high for *S. gigantea* (h_S = 0.77) associated with a highly significant structuring (Φ_{ST} = 0.651–0.715; Table 3). At the subspecies level, the highest gene diversities were found for both *S. gigantea* subspp. *gigantea* and *hellenica* (h_S = 0.80 and 0.79, respectively), followed by the Epirus group (h_S = 0.65) and *S. gigantea* subsp. *rhodopea* (h_S = 0.41).

Table 2. Diversity indices and their standard deviation for the nuclear marker (ITS) and cpDNA combined markers (*trn*H-*psb*A and *trn*S-*trn*G) for the three subspecies of *Silene gigantea* and the Epirus group.

	cpDNA				
Standard diversity indices	*gigantea*	*hellenica*	*rhodopea*	Epirus	total
Sample size	49	96	54	31	230
No. of haplotypes	8	4	5	1	15
No. of polym. loci	13	5	8	0	20
Nucleotide diversity[$] ($\pi \pm SD$)	2.43 ± 1.60	2.82 ± 1.77	2.99 ± 1.86	0	3.77 ± 2.22
Allelic richness (Rs)	1.02	1.01	1.04	1	1.55
Gene diversity ($h \pm SD$)	0.795 ± 0.030	0.643 ± 0.028	0.679 ± 0.054	0	0.873 ± 0.009
					h_S=0.036 ± 0.016
Tajima's D	-1.784	1.589	1.054	0	-1.262
Tajima's D *p*-value	0.011	0.940	0.862	1	0.054
Fu's Fs	-0.841	4.418	2.596	-	-1.015
Fs p-value	0.373	0.946	0.876	-	0.420
	ITS				
Standard diversity indices	*gigantea*	*hellenica*	*rhodopea*	Epirus	total
Sample size	35	90	47	32	204
No. of ribotypes	17	28	13	5	56
No. of polym. loci	14	19	10	4	32
Nucleotide diversity[$] ($\pi \pm SD$)	2.50 ± 1.60	2.1 ± 1.4	0.80 ± 0.70	1.50 ± 1.10	2.44 ± 1.55
Allelic richness (Rs)	1.41	1.53	1.31	1.12	1.78
Gene diversity ($h \pm SD$)	0.798 ± 0.045	0.795 ± 0.0276	0.412 ± 0.065	0.647 ± 0.052	0.774 ± 0.021
No. of heterogenous sequences	13	53	12	1	79
No. of homogenous sequences	22	37	35	31	125

[$] Figures were multiplied by 1000.

Table 3. AMOVA on ITS nuclear sequences and the cpDNA combined markers *trn*H-*psb*A and *trn*S-*trn*G according to Geneland clustering and morphology (the three subspecies + the Epirus group or the three subspecies with the Epirus group clustered within *S. gigantea* subsp. *gigantea*).

	ITS			**cpDNA**		
Clustering according to	Geneland	morphology	morphology	Geneland	morphology	morphology
Number of groups	5	4	3	5	4	3
Percentage of variation						
among groups	56.5	20.4	9.9	48.0	40.3	29.5
among pop. within groups	15.1	45.4	55.2	50.2	58.0	68.7
within populations	28.4	34.1	34.9	1.7	1.7	1.7
Φ_{ST}	0.715***	0.659***	0.651***	0.967***	0.971***	0.975***
Φ_{SC}	0.346***	0.571***	0.613***	0.983***	0.983***	0.983***
Φ_{CT}	0.565***	0.204***	0.100**	0.480***	0.403***	0.295***

, * correspond to P<0.01 and P<0.001, respectively.

The nucleotide diversities presented a similar pattern (Table 2). Ribotype richness was the highest in *S. gigantea* subsp. *hellenica* (R_S = 1.53), whereas it was the lowest in the Epirus group (R_S = 1.12). The ITS ribotype I107 was the most abundant within populations and the most geographically widespread (see Appendix 5).

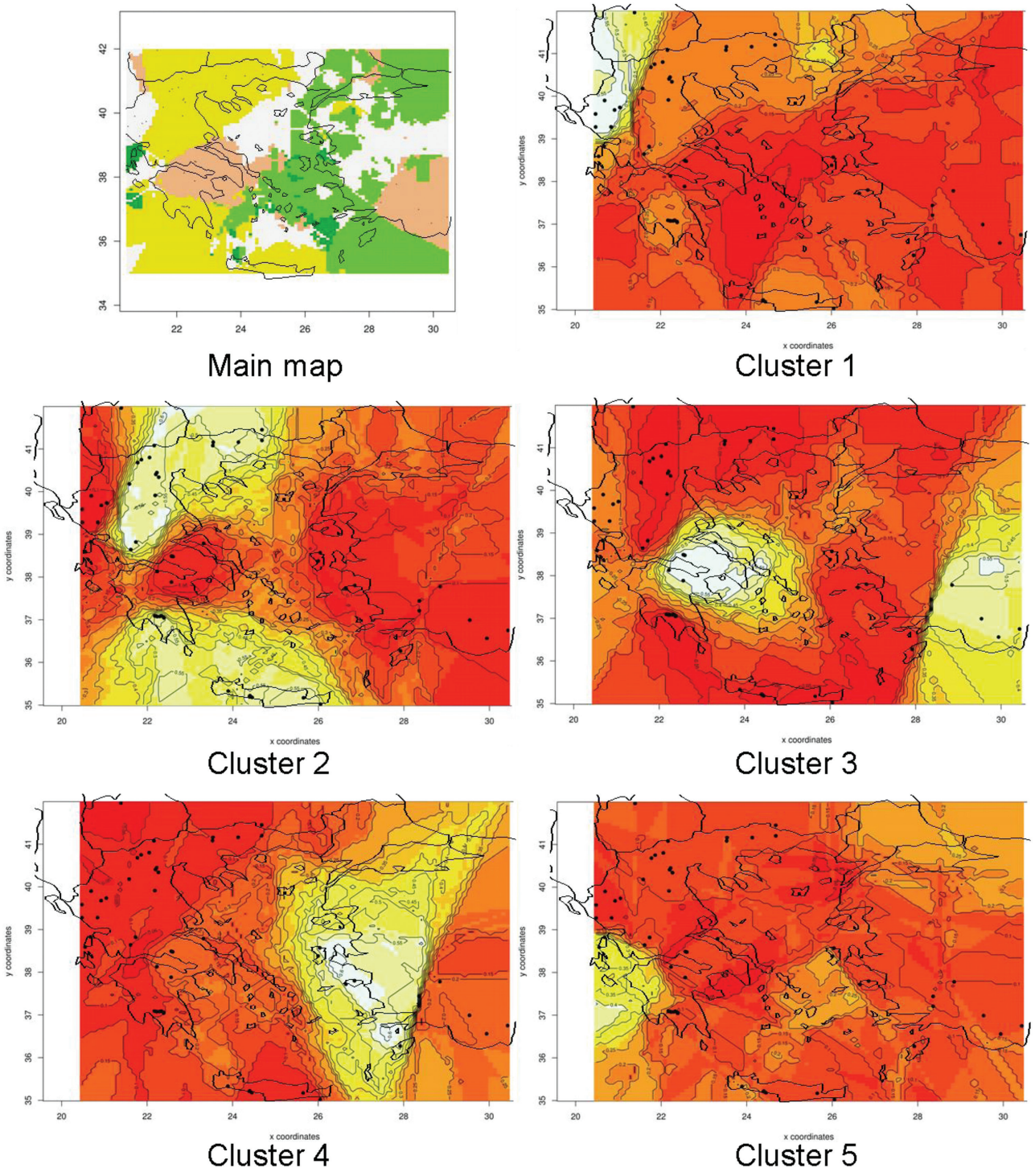

Figure 1. Maps of ITS cluster memberships with posterior probability for each cluster based on Geneland analyses of *Silene gigantea*. Colours indicate the region of high (light yellow) to low (red) posterior probability of membership to a given cluster. The Mediterranean area contours are given in blue. The scales correspond to the longitude and latitude.

ITS GENETIC CLUSTERING

The 20 independent runs of Geneland on ITS sequences all revealed the same five genetic clusters (Fig. 1). Cluster 1 comprised all populations from the Epirus region in north-western Greece and matches the ambiguous morphogroup of Epirus. Populations

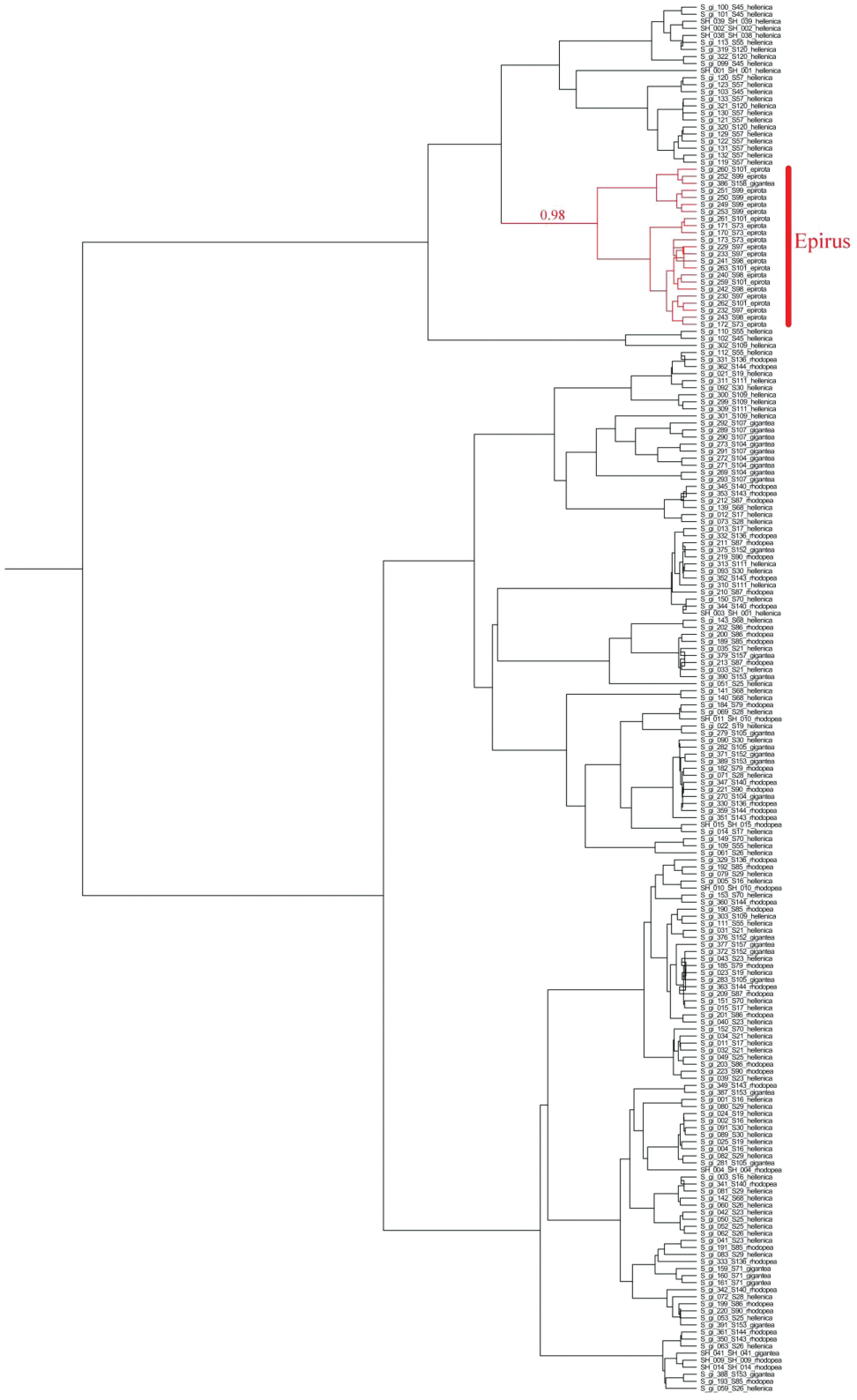

Figure 2. ITS maximum credibility clade tree obtained with BEAST version 1.8.2 on 197 individuals of *Silene gigantea*. The red clade corresponds to individuals from the Epirus region (north-western Greece) and one individual from Lefkas identified as *S. gigantea* subsp. *gigantea*. Posterior probabilities that are equal or higher that 0.50 are given above the corresponding branches.

from Crete, north-central Greece and the southern Peloponnese were grouped together in cluster 2. Cluster 3 included populations from eastern Sterea Ellas, northern Peloponnese and all Turkish populations. Populations from the Dodecanese formed the fourth cluster. The fifth included populations from the island of Lefkas. The ITS species tree (Fig. 2) does not support the different subspecies of *S. gigantea* or any geographical structuring with the exception of all individuals from Epirus, which form a strongly supported clade (posterior probability, PP = 0.98). This is due to the presence of several private ribotypes in those populations. However, one individual from Lefkas (near to Epirus populations) identified as *S. gigantea* subsp. *gigantea* also belongs to this clade.

Plastid diversity and overall differentiation

Two hundred and forty-two individuals from 59 populations were sequenced for HA (4.10 ± 1.86 individuals per population) and 231 individuals from 58 populations were obtained for SG (3.98 ± 1.79 individuals per population). HA and SG haplotypes contained six and four indels, respectively, with the lengths of 21, 21, 13, 9, 6 and 15 bp and 6, 13, 6 and 5 bp, respectively. Few substitutions were recorded with three polymorphic sites in HA and one in SG. One inversion (56 bp) was also recorded in HA. HA appeared slightly more diverse than SG, with ten vs. four haplotypes. The combination of HA and SG led to 14 haplotypes (229 individuals from 60 populations; Table 2; Fig. 3). Nearly all populations with at least two individuals (91.0%) were monomorphic except four, found on mainland, which

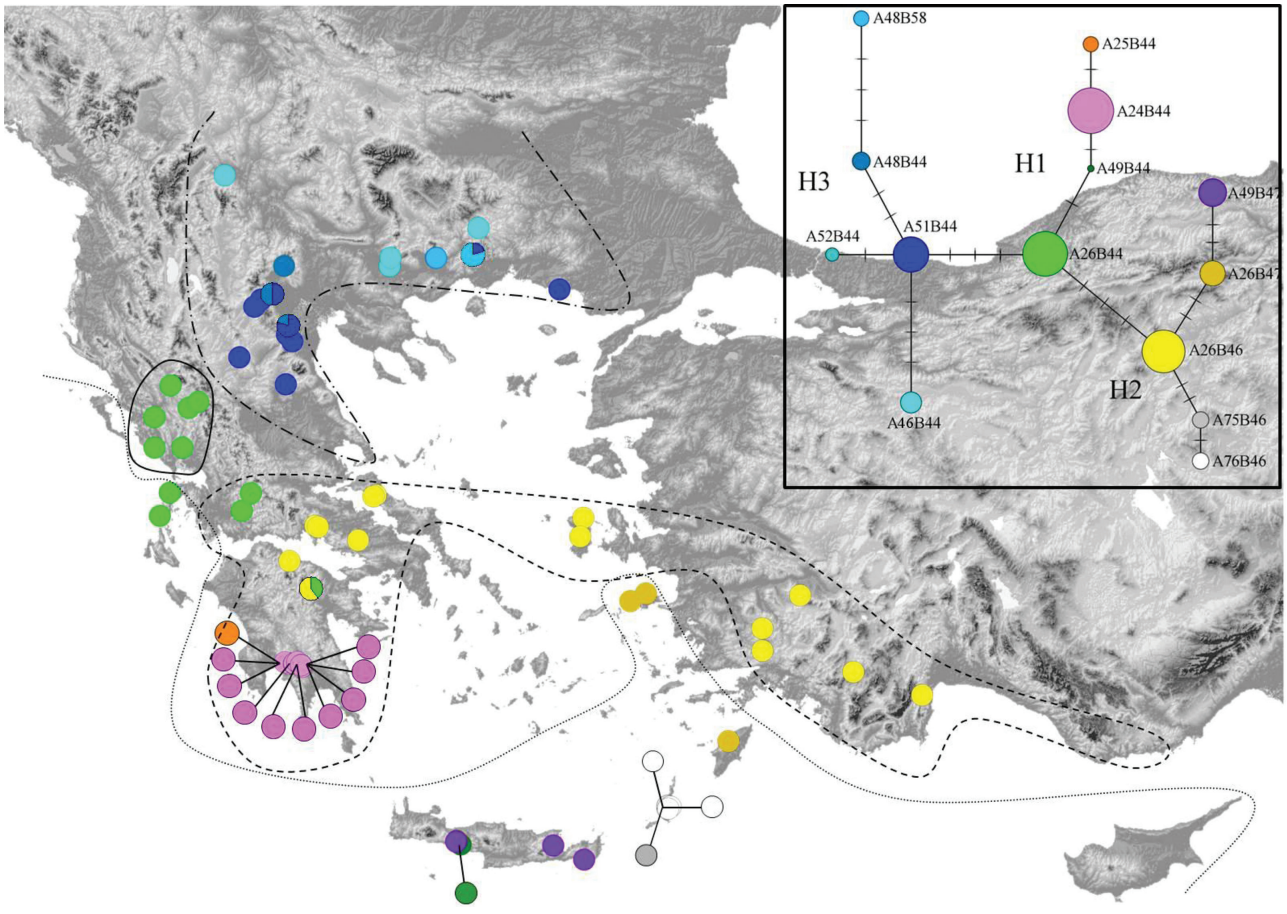

Figure 3. Distribution map of the 14 *trnH-psbA* (HA) and *trnS-trnG* (SG) concatenated haplotypes. *Silene gigantea* subsp. *rhodopea* occurs north of the broken-and-dotted line, *Silene gigantea* subsp. *hellenica* occurs within the broken line, *Silene gigantea* subsp. *gigantea* occurs south of the dotted line, and the Epirus group occurs within the solid circle. The median joining network of plastid combined haplotypes for 229 individuals is shown at the top right. The size of each haplotype is proportional to its frequency within the species. Mutational steps are indicated as dashes. Group H1 corresponds to the yellow, gold, purple, grey and white haplotypes; group H2 to the green, pink and orange haplotypes and group H3 to all blue haplotypes.

displayed two haplotypes each. Consequently, the haplotype diversity per population was low (h_s = 0.036 ± 0.016), whereas the overall haplotype diversity was high (h_t = 0.868 ± 0.016), leading to high Φ_{ST} values (0.967–0.975; Table 3). All neutrality tests (Tajima's D and Fu's F_S) were nonsignificant for the different groups (*P*-value > 0.05) except for *S. gigantea* subsp. *gigantea* (Tajima's D = –1.78; *P*-value = 0.0114).

Plastid network

The relationships among the 15 plastid DNA haplotypes are shown in Fig. 3. One to three mutational steps are found between pairs of haplotypes. Figure 3 also shows that haplotypes distribution matches with geography. Using both network topology and haplotypes distributions, three main groups could be drawn: H1 (A26B44, A49B44, A24B44 and A25B44), H2 (A26B46, A26B47, A49B47, A75B46 and A76B46) and H3 (A51B44, A52B44, A46B44, A48B44 and A48B58). H1 includes four haplotypes occurring in the southern Aegean Island Arc with A24B44 and A25B44 found in the Taygetus Mountains (southern Peloponnese), A49B44 in eastern Crete and A26B44 in north-western Greece and Corinthia. This group includes two common haplotypes (A24B44: 19.6% and A26B44: 18.3%). H2 comprises five haplotypes with A26B46 being the most geographically widespread and also one of the most common haplotypes (19.7%) occurring on the Greek mainland (Stera Ellas, northern Peloponnese) and in Euboea, Chios and Turkey. Haplotype A26B47 was found on Samos and Rhodes, A49B47 on Crete and A75B46 and A76B46 on Karpathos. Haplotype A49 was also found in a single Turkish population in Antalya that could not be sequenced for SG. H3 displays five haplotypes only found in northern Greece, including Macedonia and north-eastern Pindus. Overall, the haplotype diversity is higher on the Greek mainland than on the Turkish mainland with nine haplotypes vs. one. Four haplotypes were restricted to the different islands of the Aegean Sea and Cyprus.

From a taxonomic perspective, the H3 group encompasses all haplotypes found for *S. gigantea* subsp. *rhodopea*, whereas haplotypes of *S. gigantea* subsp. *gigantea* and *S. gigantea* subsp. *hellenica* are found scattered in groups H1 and H2, with only one shared haplotype between them. Indeed, the Epirus population, which is fixed for A26B44, displays the same haplotype as the one found in the Ionian populations of *S. gigantea* subsp. *gigantea* (Lefkada) and in the Etolia-Acarnanian populations of *S. gigantea* subsp. *hellenica*.

Genetic vs. morphological structuring

The genetic structuring was compared among the Geneland clustering, the taxonomic delimitation into three (Epirus populations + *gigantea* – *hellenica* – *rhodopea*) and into four groups (Epirus – *gigantea* – *hellenica* – *rhodopea*) using AMOVA (Table 3). For both plastid DNA and ITS, the different *Φ*-statistics (Φ_{ST}, Φ_{SC} and Φ_{CT}) were highly significant ($P < 0.0001$). For ITS, the highest differentiation among groups (Φ_{CT}) was found for Geneland clustering (56.5% vs. 20.4% and 9.9% for the taxonomic clustering into four and three morphological groups, respectively). Both types of clustering were more similar for plastid DNA compared to ITS, with a differentiation among groups of 48.0%, 40.3% and 29.5% for the genetic and the four and three taxonomic groups clustering, respectively.

Divergence time estimates and phylogeographic patterns

The two plastid phylogenetic trees obtained without and with geographical constraints are shown in Figures 4 and 5, respectively. Both trees clearly suggest a post-Messinian diversification. The ancestral node age differs between the two analyses, although not significantly so. Time estimates point to the Pleistocene from 1.20 Myr (95% HPD interval = 0.36–2.92) to 1.51 Myr (0.45–3.51) (Figs 4 and 5, respectively). This age is recent considering that of Sileneae, estimated to range from 20 to 27 My (Frajman *et al.*, 2009; Sloan *et al.*, 2009). Clade compositions are congruent, but tree topologies and clade supports differ between analyses. This is expected since the addition of localities as a trait highly constrains tree reconstruction. In general, higher supports were found when including geography as a trait. *Silene gigantea* subsp. *rhodopea* forms a well-supported clade (posterior probability, PP ≥ 0.97), with a divergence estimated *c*. 1.20 (95% HPD interval = 0.36–2.93) or 0.77 Myr (HPD interval = 0.001–1.06) depending on the tree. However, the relationship of this clade with the others is poorly supported and differs also between analyses. *Silene gigantea* subspp. *hellenica* and *gigantea* are clearly polyphyletic, with well-supported clades, at least in Figure 5, each comprising individuals from small and well-defined geographical areas. The Epirus group clusters with the Ionian populations of *S. gigantea* subsp. *gigantea* and some individuals belonging to *S. gigantea* subsp. *hellenica* from central western Greek mainland. It forms a moderately supported clade in both trees (0.50 and 0.88, respectively). Again, its relationship to the other clades differs depending on the tree. When geography is taken into account, the southern populations of *S. gigantea* subsp. *hellenica* form a well-supported clade (PP = 0.96; Fig. 5), which is sister to a population from western Crete. Other populations of *S. gigantea* subsp. *hellenica* (central-western Greek mainland, northern Peloponnese, Euboea, Chios and south-western

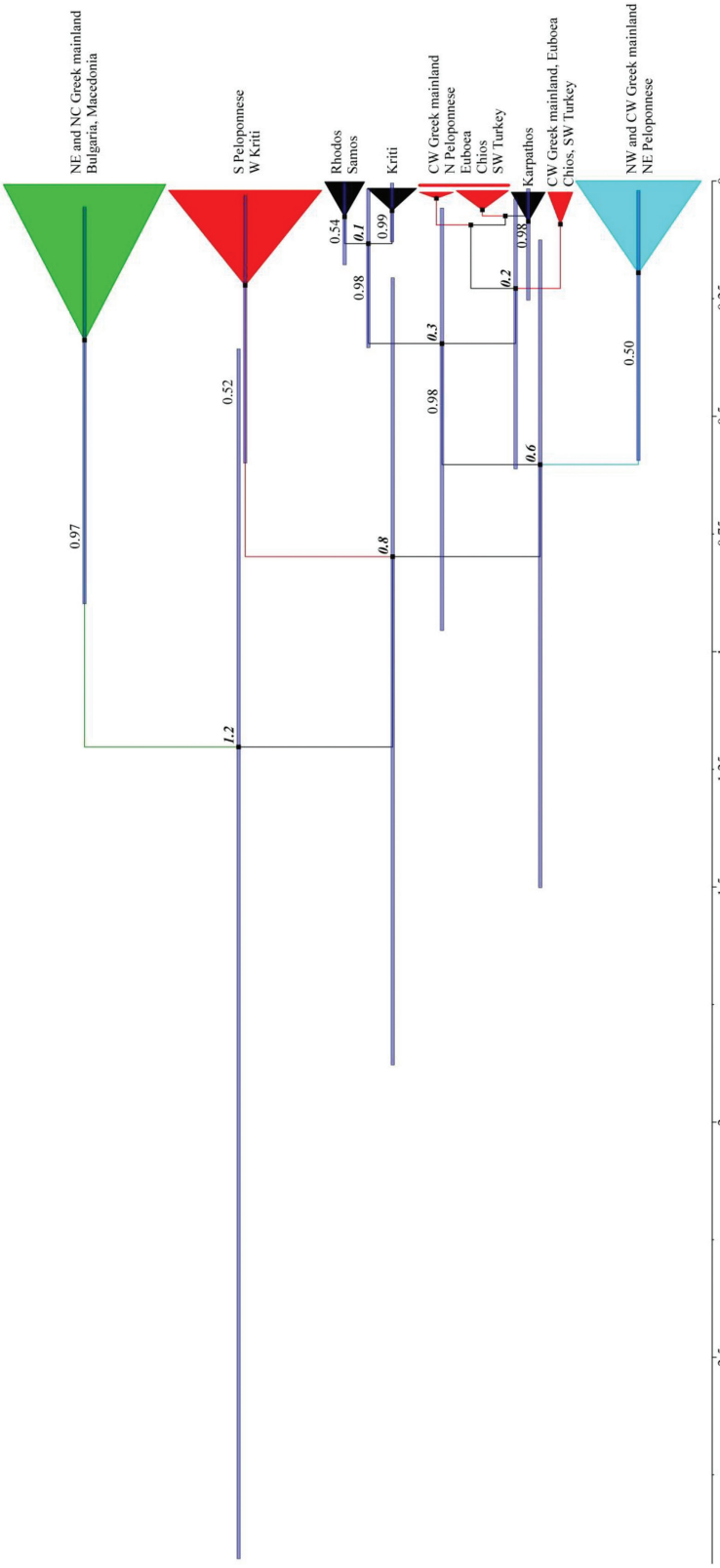

Figure 4. Bayesian maximum credibility clade tree based on the combined *trnH-psbA* (HA) and *trnS-trnG* (SG) plastid markers for *Silene gigantea*. The posterior probabilities equal to or higher that 0.50 are given above the corresponding branches. The divergence times (in Myr) are given at the nodes in italic and bold. The node bars represent the standard deviation for time estimates. *Silene gigantea* subsp. *rhodopea* is highlighted in green, *S. gigantea* subsp. *hellenica* in red and *S. gigantea* subsp. *gigantea* in black. The Epirus group comprising related populations such as the Ionian individuals of *S. gigantea* subsp. *gigantea* and central-western individuals of *S. gigantea* subsp. *hellenica* are highlighted in blue. The scale is given in million years (Myr).

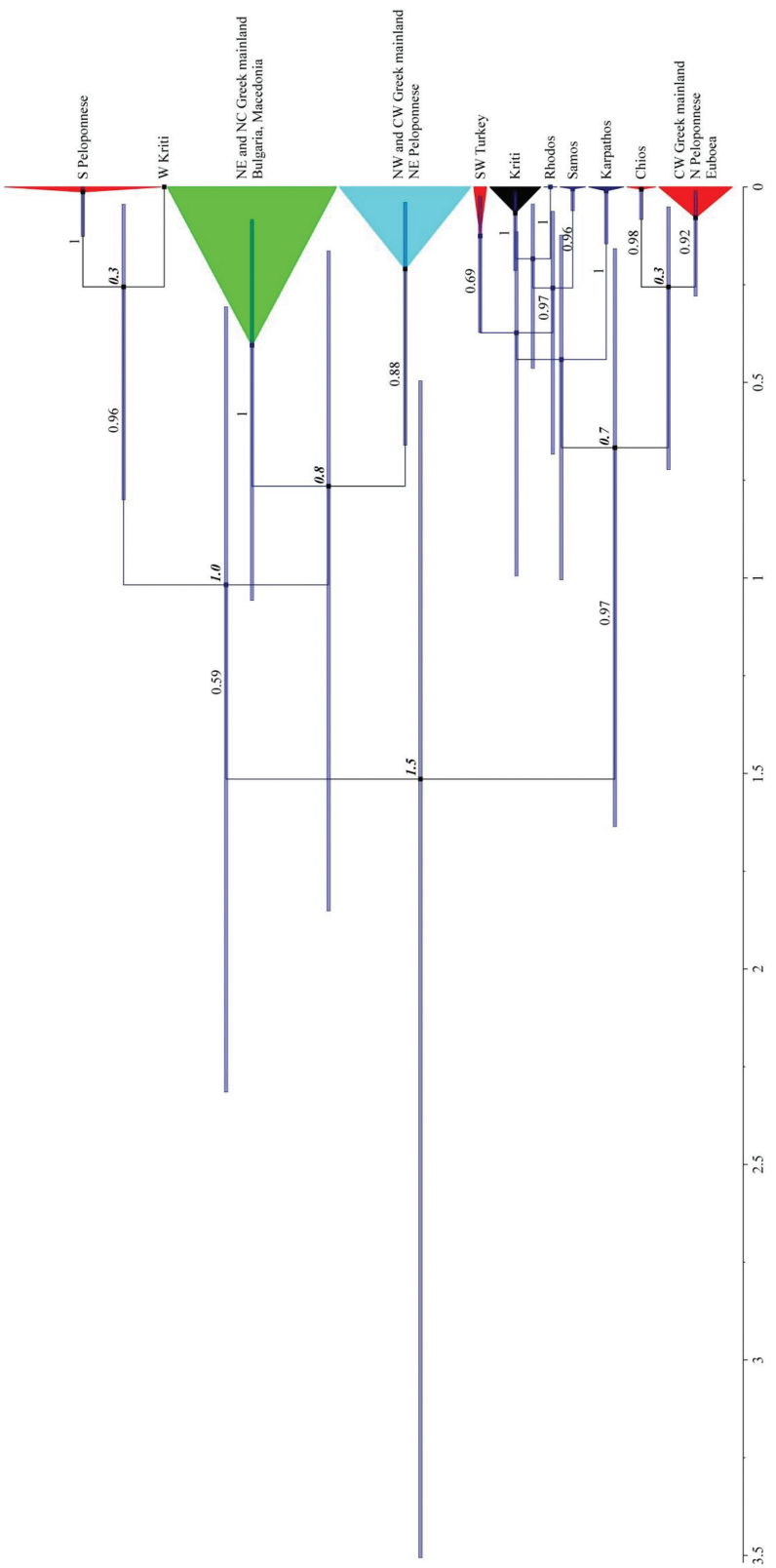

Figure 5. Bayesian maximum credibility clade tree taking into account geolocated data in addition to the combination of the two plastid markers *trnH-psbA* (HA) and *trnS-trnG* (SG) for *Silene gigantea*. The posterior probabilities that are equal to or higher that 0.50 are given above the corresponding branches. The divergence time (in Myr) is given at the nodes in italic and bold. The node bars represent the standard deviation for time estimates. *Silene gigantea* subsp. *rhodopea* is highlighted in green, *S. gigantea* subsp. *hellenica* in red and *S. gigantea* subsp. *gigantea* in black. The Epirus group comprising related populations such as the Ionian individuals of *S. gigantea* subsp. *gigantea* and central-western individuals of *S. gigantea* subsp. *hellenica* are highlighted in blue. The scale is given in million years (Myr).

Turkey) are either scattered in several non-supported clades (Fig. 4) or clustered into three relatively well-supported geographical clades (Fig. 5). Within *S. gigantea* subsp. *gigantea*, populations from Karpathos form a clade that is distant from all other populations of the southern Aegean area in both trees (Crete, Rhodes and Samos).

The MCC tree-based phylogeographic reconstruction (Fig. 6) represents the diffusion of *S. gigantea* through space and time. The ancestral area is estimated to have occurred in the central Greek mainland, from where two lineages started to spread. The first one expanded to the north-west and rapidly divided and colonized the northern Balkan Peninsula (*S. gigantea* subsp. *rhodopea*) and the west (Epirus and Ionian area). The second lineage expanded on the one hand to the east and colonized the eastern Aegean area and south-western Turkey and, on the other hand, to southern Greece. The migration from Greece to Turkey started earlier (1.00–0.45 Myr) than the colonization of Crete (0.20–0.03 Myr). On Crete, two separate colonization events were evidenced, one from the west and one from the east (Fig. 6).

DISCUSSION

The plastid DNA loci (HA and SG) and the nuclear marker (ITS) used in the present study were informative enough to investigate the phylogeography of the *S. gigantea* complex. The genetic structure was higher for the plastid spacers than for the nuclear marker, but this is a common pattern due to the low diversity found within populations for the former loci. Such contrasting values also are found in the Aegean *Nigella arvensis* L. complex (Bittkau & Comes, 2005) and in the Cretan chasmophyte *Brassica cretica* Lam. (Edh, Widén & Ceplitis, 2007). Overall, plastid DNA sequences revealed a higher diversity on the Greek than on the Turkish mainland.

The genetic results using plastid DNA are partly congruent with the morphological classification of Greuter (1995, 1997) and Du Pasquier *et al.* (2015). Accordingly, *S. gigantea* subsp. *rhodopea* is monophyletic, whereas *S. gigantea* subspp. *gigantea* and *hellenica* are polyphyletic. The hybrid origin of the Epirus group is not supported, which confirms the hypothesis of Du Pasquier *et al.* (2015), but the phylogenetic analyses suggest a geographical isolation of the group from mainland populations in contradiction with Du Pasquier *et al.* (2015) who assumed an island origin for the group. A genetic continuity between central-eastern Greece and south-western Turkey is also revealed and at least two independent colonizations of Crete are suggested. These oversea connections are estimated to be of post-Messinian origin (Pleistocene). Such

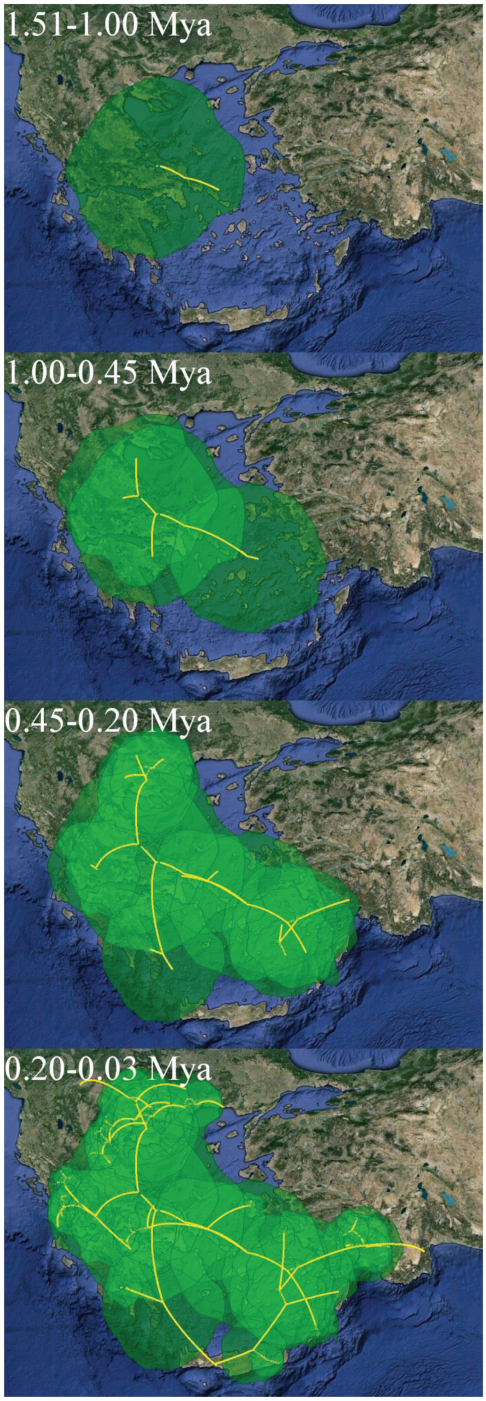

Figure 6. Screenshots of the main steps of the phylogeographic history of *Silene gigantea* across the Balkan Peninsula and south-western Turkey based on the analysis of the combined plastid regions *trnH-psbA* and *trnS-trnG* using SPREAD. Yellow lines represent the branches of the MCC tree (Fig. 4). The green polygons represent the ancestral nodes areas (80% highest posterior density areas) at the different time periods as indicated in the upper left side. The projection was performed using Google Earth.

colonization events linking both sides of the Aegean (Greece and Turkey) during the Quaternary era cannot be related to the palaeogeographic history of the region and the main geological events that shaped the current Aegean topography, that is the mid-Aegean trench (MAT) and the Messinian salinity crisis (MSC), which are widely recognized to have occurred earlier, that is *c*. 10 and 6 Myr, respectively (Suc & Clauzon, 1996; Perissoratis & Conispoliatis, 2003; Krijgsman *et al.*, 2010; Poulakakis *et al.*, 2015).

Taxonomic vs. phylogeographic delimitation

As observed from the AMOVA results, the ITS clustering is not consistent with the taxonomic delimitation at the subspecies level, probably due to the sharing of the putative ancestral ribotype I107 in all subspecies (Appendix 5) and to incomplete lineage sorting. Conversely, the results based on the two plastid markers are partly concordant with the current taxonomic delimitation (Greuter, 1995, 1997; Du Pasquier *et al.*, 2015). *Silene gigantea* subsp. *rhodopea* is monophyletic (Figs 4 and 5) and only displays plastid DNA haplotypes that are private to it (haplotype group H3; Fig. 3). This finding contradicts previous studies reporting that *S. gigantea* subsp. *rhodopea* exists in Turkey (Coode & Cullen, 1967; Yıldız & Çırpıcı, 2013). The Turkish populations proved to be genetically different from those of *S. gigantea* subsp. *rhodopea*, but identical to populations from the central-eastern Greek mainland using both ITS and plastid DNA markers (Figs 1 and 3). The assessment, based on morphology (Du Pasquier *et al.*, 2015), that only *S. gigantea* subsp. *hellenica* is present in Turkey is thus confirmed in this work.

In contrast, *S. gigantea* subspp. *gigantea* and *hellenica* are polyphyletic according to plastid DNA analyses. This finding highlights the strong morphological plasticity that exists within the complex and suggests cases of morphological convergence between islands and the mainland. Indeed, *S. gigantea* subspp. *gigantea* and *hellenica* are mainly distinguishable morphologically, due to their differing inflorescence shape, indumentum on the calyx and number of flowers (see Du Pasquier *et al.*, 2015). Some exceptions exist, as for populations from Chios and Euboea, which were not clearly determined using morphological characters (Du Pasquier *et al.*, 2015). These populations display the same haplotype as the Turkish and eastern central Greek ones and could therefore be classified as *S. gigantea* subsp. *hellenica*.

Finally, no direct genetic relationship is found between populations from the southern Peloponnese (Taygetus Mountains) and those from the northern Peloponnese. These groups of populations, which are morphologically similar and identified as belonging to the *S. gigantea* subsp. *hellenica*, display divergent plastid DNA haplotypes (groups H1 and H2, respectively; Fig. 3) and are clustered into two different clades (Figs 4 and 5). Populations from the Taygetus Mountains (southern Peloponnese) appear to be genetically related to populations from Crete (*S. gigantea* subsp. *gigantea*), whereas populations from the northern Peloponnese are identical to populations from Sterea Ellas and Turkey (*S. gigantea* subsp. *hellenica*). Clear links in species composition between Mount Taygetus and Crete on the one hand and between the northern Peloponnese and Sterea Ellas on the other have been shown for many other taxa (Dimopoulos & Georgiadis, 1992). The same observation holds for populations from the southern Hellenic Arc belonging to *S. gigantea* subsp. *gigantea* since populations from Karpathos are not directly related to populations from Crete and Rhodos. Thus, we assume that island conditions and chasmophytic ecology strongly select for specific morphotypes, corresponding to the *S. gigantea* subsp. *gigantea* habit. This might have been enabled by a large morphological plasticity (see Du Pasquier *et al.*, 2015 for morphological details), which is recurrently found in *Silene* (Frajman & Oxelman, 2007; Đurović *et al.*, 2017).

Greuter (1995, 1997) reported that populations from the Epirus region exhibit mixed morphological features and are therefore probable hybrids or introgressed individuals of *S. gigantea* subspp. *gigantea* and *rhodopea*. Our study suggests an alternative scenario. No direct genetic relationship between the Epirus populations and individuals of *S. gigantea* subsp. *rhodopea* was found using ITS and plastid DNA loci, whereas only one ribotype (ITS) is shared with the Ionian populations identified as *S. gigantea* subsp. *gigantea* (Fig. 2l; Appendix 5). Populations from Epirus cluster separately in the ITS analyses (Cluster 1, Figs 1 and 2), indicating limited gene flow and isolation from other mainland populations. This pattern is also inferred by plastid DNA, in which all Epirus populations are fixed for a single haplotype, shared however with the Ionian populations of *S. gigantea* subsp. *gigantea* and central-western populations of *S. gigantea* subsp. *hellenica*. According to the phylogeographic analyses, the Epirus group seems to have diverged quite early in north-western Greece. The Ionian populations of *S. gigantea* subsp. *gigantea* probably resulted from a colonization from mainland, in contradiction with Du Pasquier *et al.* (2015) who assumed a colonization of the Epirus region from the Ionian Islands.

The Epirus populations are morphologically different from the three other subspecies, as already assessed by Du Pasquier *et al.* (2015), and are genetically differentiated as a well-supported clade for the nuclear marker. The situation is fuzzier for the plastid markers, as haplotype A26B44 characterizing the Epirus populations is also found in the eastern and southern

populations, respectively, Lefkas Island and western Greece + north-eastern Peloponnese (Fig. 3). This could however be due to plastid capture following population admixture (Soltis & Kuzoff, 1995; Naciri & Linder, 2015). For all these reasons and as nuclear markers were shown to better translate species boundaries than plastid ones when seed disersal is limited (Naciri, Caetano & Salamin, 2012), we propose to consider the Epirus populations as belonging to a new subspecies *S. gigantea* subsp. *epirus* described below.

A recent evolutionary history

Most of the phylogeographic studies in the Aegean area reveal vicarious processes with a distributional break between the western and eastern Aegean. Such a break is usually related to the formation of the MAT (9–12 Myr), which corresponds to the first separation of Greece and Turkey (Poulakakis *et al.*, 2015). In contrast, our study shows a genetic continuity across the Aegean Sea, supported by ITS and plastid sequences and by morphological features (Du Pasquier *et al.*, 2015). Oversea long-distance dispersal seems unlikely (Fig. 3) although it cannot be completely excluded. Human translocation can also be excluded, since no recent introduction was evidenced on the Aegean Islands. Our data therefore suggest that the colonization of different areas implied relatively recent continuous populations through the Kyklades Islands, which could have acted as stepping-stones. Indeed, the time of the most common ancestor coincides closely with the ice ages of the Quaternary period (Figs 4 and 5). Klopfstein, Currat & Excoffier (2006) demonstrated that large areas with a single haplotype can result from a process of surfing on the wave of a spatial expansion. The negative and significant Tajima's D for *S. gigantea* subsp. *gigantea* can be either interpreted as the footprint of a population expansion after a recent bottleneck (Klopfstein *et al.*, 2006) or a sign of a recent selective sweep (Percy *et al.*, 2014). Both scenarios can mimic a range expansion with haplotype surfing.

Migration from Greece to eastern Aegean area and south-western Turkey

Considering our hypothesis, eustatic processes ensured cyclic connections between islands and the mainland via periodic land bridges during the Quaternary. Consequently, the sea level varied considerably between the glacial and interglacial stages during the Pleistocene (Perissoratis & Conispoliatis, 2003). The Aegean Sea bed probably emerged due to shallowness (Brosolo, Mascle & Loubrieu, 2012), which might have allowed for the dispersal of *S. gigantea*. The current absence of *S. gigantea* from most of the Kyklades ('Cycladean gap') and the Sporades Islands might result from the palaeogeographic changes and climatological alterations during the Quaternary period as mentioned by Dimopoulos & Georgiadis (1992). The records of *S. gigantea* on Alónnisos (Sporades) and Anáfi (Kiklades) (Greuter, 1997; Strid, 2016) probably represent remnants of such dispersals, although the presence of *S. gigantea* on those islands still needs to be confirmed.

Two colonization events for Crete

The latest land bridges between Crete and the Peloponnese are assumed to have occurred during the MSC, that is 5.3–5.5 Myr (Greuter, 1970; Cellinese *et al.*, 2009; Simaiakis *et al.*, 2012; Poulakakis *et al.*, 2015), but our data show that *S. gigantea* colonized Crete well after this period (<1 Myr from our estimates), through at least two separate colonization events (Fig. 6) which occurred at approximately the same time period. The first route most probably involved a western connection between Crete and the southern part of Peloponnese. Gielly, Debussche & Thompson (2001) and Thompson (2005) reported a similar pattern for closely related Peloponnesian and Cretan populations in the *Cyclamen repandum* Sm. complex (Primulaceae). This might be explained by a long-distance dispersal event or by a stepping-stone colonization involving the islands of Kithera and Antikithera between Crete and the Peloponnese, although *S. gigantea* is not present on those islands. The southern Peloponnesian populations apparently did not move further north and were then isolated in the gorges of the Taygetus Mountains (see above) and probably also in the lower mountains of Parnon (south-eastern Peloponnese), which acted as an endemism centre for many species (Trigas *et al.*, 2012). Colonization toward the northern Peloponnese from Taygetan populations was prevented either by the isolation of the southern Peloponnese during the glacial periods or by the Korinthiakos Gulf behaving as a natural barrier (Strid, 1986).

The second colonization of eastern Crete is revealed at approximately the same period (Figs 4–6). The corresponding Cretan populations are closely related to populations on Rhodes and Samos (divergence *c.* 0.36 Mya), whereas the populations of Karpathos are closer to the Turkish populations (divergence *c.* 0.38 Mya). Similar unexpected patterns on Karpathos have already been discussed by several authors (Gantenbein & Keightley, 2004; Bittkau & Comes, 2005; Parmakelis et al., 2006a, b), whereas it is assumed that Karpathos was connected to Rhodes and the Turkish mainland 3.2 Mya, that is in the early Pliocene (Poulakakis *et al.*, 2015) and has been isolated since then (Creutzburg, 1958).

Colonization of Cyprus

The origin of lineages on Cyprus of many taxa (mainly animals) remains unclear. If connections of the island with the mainland followed by isolation and vicarious events are assumed by most authors for animals (Gantenbein & Keightley, 2004; Poulakakis et al., 2005, 2013; Sevgili *et al.*, 2006; Parmakelis *et al.*, 2006a; Lymberakis *et al.*, 2007; Akın *et al.*, 2010; Kornilios *et al.*, 2012; but see Dermitzakis, 1990), the frame time of such events fluctuates between 10 Mya (before the MAT) and 5.33 Mya (just after the MSC). However, more recent colonizations of Cyprus by herptiles in the Pliocene and Pleistocene are reported (Lymberakis *et al.*, 2007; Poulakakis *et al.*, 2013) and in the case of *Euphorbia lemesiana* Hadjik., Hand, Christodoulou & Frajman (Hand *et al.*, 2015) but without satisfactory palaeogeographic explanations. Therefore, the current restricted distribution of *S. gigantea* on the northern calcareous slopes of the Pentadaktylos range in Cyprus suggests a probable colonization from Turkey. This should however be tested using better sampling.

Diversification in the northern Balkan peninsula

Possible reasons for the genetic diversification within *S. gigantea* subsp. *rhodopea* (haplotype group H3) can be related to spatial or demographic expansion during interglacial stages, with the colonization of new ecological niches as suggested by the siliceous habitat of some populations. A second hypothesis is related to the northern part of Balkan Peninsula being recognized as an important refuge during the Pleistocene glacial cycles with climatic fluctuations causing species invasions and retreats (Comes & Kadereit, 1998; Triantis & Mylonas, 2009). Thus, the Bulgarian and Serbian populations could have found refuge in northern Greece, something that would explain the numerous haplotypes present in Thrace. Finally, a putative route of colonization across the Bosphorus is refuted, and it can be assumed that *S. gigantea* subsp. *rhodopea* was stopped during its expansion in the southern Rhodopes Mountains.

CONCLUSIONS

Our study of *S. gigantea* remains somewhat speculative since it did not include populations from all possible regions. Evidence was found for a strong morphological convergence between *S. gigantea* subspp. *gigantea* and *hellenica* under similar ecological pressures, including the chasmophyte life-form. The analyses point to a relatively recent evolutionary divergence of the species. The history of *S. gigantea* involves recent connections between areas unanimously recognized as disjunct since a long time. Such a pattern is not, however, an isolated case. Recent studies in the western Mediterranean (Stöck *et al.*, 2008; Troia, Raimondo & Geraci, 2012; Hand *et al.*, 2015) have indeed shown connections between Sicily and the African mainland or between Cyprus and the mainland more recently than what was usually, and until now, assumed by geologists. The molecular and morphological continuity found across the Greek and Turkish populations of *S. gigantea* points to a relatively recent connection between the two areas. Factors involved in these processes could be linked to the glacial and interglacial events of the Quaternary or to long-distance dispersal events. Our lack of sampling on Cyprus did not allow us to explore this part of the history of *S. gigantea*, which remains to be investigated. Finally, this work highlights the need for comparative phylogeographic studies in order to gain confidence on the different colonization hypotheses in space and time. Several taxa, not studied so far to our knowledge, display a similar geographical pattern to that of *S. gigantea*, such as *Potentilla speciosa* Willd. (Ranunculaceae), *Convolvulus libanoticus* Boiss. (Convolvulaceae), *Astragalus angustifolius* Lam. (Fabaceae), *Telephium imperati* subsp. *orientale* (Boiss.) Nyman (Molluginaceae) and *Acantholimon echinus* Boiss. (Plumbaginaceae); these taxa deserve further investigation.

TAXONOMIC TREATMENT

Silene gigantea **subsp.** *epirota* Du Pasquier, subsp. nov.

Type

Holotype: [Greece, Epirus, Ioannina] ‘sur la route longeant le lac de Ioannina par l’E’ ‘on the road alongside the Ioannina lake from the East’, 700 m, 11 June 2011, *Du Pasquier, P.-E., C. Christe and M. Esmerode 148* (holotype: G!).

Diagnosis

Differs from *S. gigantea* subsp. *rhodopea* (Janka) Greuter by its eglandular calyx, pedicels and bracts and by its basal leaves usually 50–85 mm long.

Description

Biennial or monocarpic perennial herb, usually chasmophytic, entirely eglandular pubescent, 110–140 cm tall, 4.5–9.5 mm of diameter at the second basal internode. *Stem* with a dense and pilose indumentum on five or six lowest internodes (hairs 0.2–0.4 mm), viscid-sticky upper internodes, 10–13 increasing (or slightly irregular) internodes below the inflorescence,

sometimes branching from the base. *Basal leaves* green or withered at anthesis, spathulate or obovate attenuated, pubescent on two faces, densely white-ciliate along undulate margin. *Caulinar leaves* usually with a glabrous adaxial surface, the lower leaves with pubescent abaxial surface and short ciliate margin, the upper leaves almost entirely glabrous, leaves at the second node obovate attenuate, 50–95 × 15–25 mm. *Main inflorescence* 4.5–11.0 × 2–8 cm, with zero to two internodes, 1–50 mm between the upper node and the prophylls of the terminal dichasia, upper nodes sometimes contracted in verticillasters of less than ten flowers. *Subthyrsoids* on four nodes or more below the main inflorescence, in a lax pyramidal panicle. *Pedicel* pubescent, 3.5–13.0 mm. *Accessory cymes* usually present in upper nodes. *Bracts* glabrous, with villous margin at the base. *Flowers* vespertine, nodding at anthesis. *Calyx* eglandular pubescent (hairs 0.3–0.5 mm), glabrous on the internal side, 8–10 mm long, 1.5–3.5 mm in the maximum width, 1.0–1.5 mm in the proximal part. *Petal* brown-greenish abaxial surface, nerves more deeply coloured, whitish adaxial surface, bifid almost to base in two obovate attenuate lobes, auricle present but not marked, glabrous or sometimes with some long hairs, claw exserted 5.5–8.5 mm long, limb 3–6 mm long, teeth triangular or ovate with densely ciliate broad margin. *Anthophore* densely pubescent, 3–4 mm long. Stamens exceeding petals, anthers first white then green at anthesis, filament 10–11 mm long. *Fruit* oblong, 9–11 × 5.5–7.0 mm, three to four times as long as anthophore. *Seeds* blackish, reniform or almost orbicular, concave lateral faces, 1.0–1.6 × 0.8–1.2 mm. *Test cells* elongate-polygonate, suture line digitate-sinuous, usually without tubercle. *Seed back* concave, clearly winged, with cells elongate and short tubercle in the central part.

Image

A scan of the type specimen is given in Fig. 7.

Distribution

Silene gigantea subsp. *epirota* appears to be restricted to the Epirus region in north-western Greece (Fig. 8). It probably extends to southern Albania.

Etymology

Named after Epirus, a historical region shared between Greece and Albania.

The key to the four subspecies of the *S. gigantea* complex is modified from Greuter (1995). For the taxonomic treatment of *S. gigantea* subspp. *gigantea*, *hellenica* and *rhodopea*, see Greuter (1995, 1997).

1. Calyx with minute (<0.08 mm), often subsessile glands, lacking eglandular hairs, inflorescence regular, compound, lax conical diplothyrsoid (stony slopes; northern Greece, Bulgaria, Macedonia, Serbia and probably Albania).....subsp. *rhodopea*

- Calyx with coarse (>0.08 mm) glandular and/or eglandular hairs; inflorescence less regular, flowers at least partly in condensed verticillasters.....2

2 Verticillasters six- to ten-flowered, rosette leaves mostly withered at flowering 3

- Most verticillasters more than ten-flowered; Hairs on calyces and pedicels mostly eglandular or

Figure 7. Holotype of *Silene gigantea* subsp. *epirota* Du Pasquier (G).

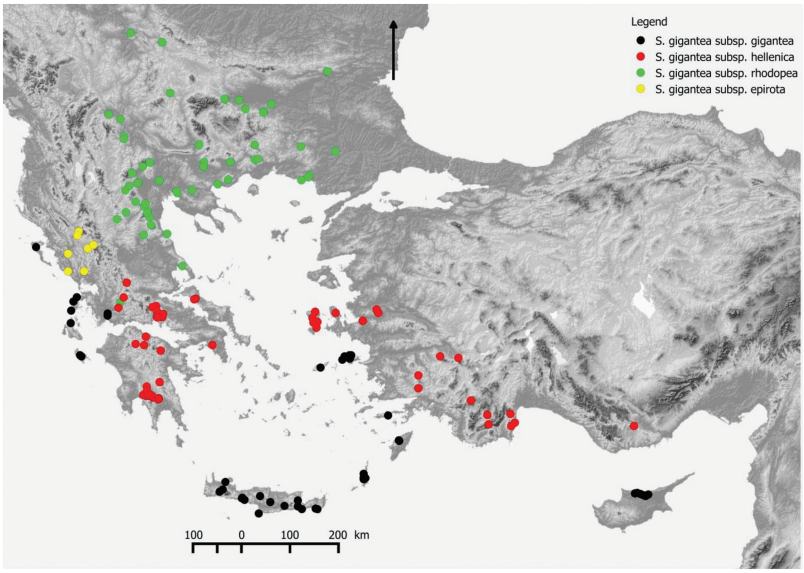

Figure 8. Distribution map of the *Silene gigantea* complex.

mixed, rarely all glandular; rosette leaves greening throughout the flowering period (limestone cliffs; western central Greece (Gorge of Kleisoura), Ionian and Aegean islands; Cyprus)…….. ……..…….....subsp. *gigantea*

3 Hairs on calyces and pedicels all glandular; (limestone cliffs; central Greece except in the west, Peloponnisos, Evvia; south-western Anatolia)……..... subsp. *hellenica*

- Hairs on calyx, pedicels and bracts all eglandular; (cliff crevices; endemic from Epirus with probable extension to south-western Albania)…..……..subsp. *epirota*

(The taxonomy of some individuals from western Etolia-Acarnania with mixed indumentum on calyx remains to be clarified).

ACKNOWLEDGEMENTS

We are indebted to Régine Niba and Maria Holzmann for their help with laboratory work, to André Schlüssel, Aurélie Cusin, Camille Christe, Manuela Esmerode and Laurence Fazan for their help with field work in Greece and to Stephan Nylinder for his help with BEAST analyses. We express our thanks to Jacques Zaffran from Kolimpari for welcoming us into his herbarium, Kemal Yıldız from Izmir for specimen loans and for his help in drafting a collection permit request and Cyrille Chatelain for his help with the map. We are also indebted to the curators of AIX, ATH, ATHU, BEI, BP, MAIC, MJSD, P, PAL, SO, W and Z herbaria who welcomed us or sent us specimens, especially Christina Fournaraki and Panagiota Gotsiou from Crete. We greatly thank Božo Frajman, Arne Strid and an anonymous reviewer for their valuable comments that improved an earlier version of this manuscript. We are especially grateful to the Greek Ministry of Environment Energy and Climatic Change for having provided the collection authorizations. Field trips were supported by the Société de Physique et d'Histoire Naturelle (Augustin Lombard travel fund) and the Société Académique de Genève (travel fund).

REFERENCES

Akın C, Beerli P, Westaway R, Ohst T, Litvinchuk SN, Uzzel T, Bilgin M, Hotz H, Guex GD, Plötner J. 2010. Phylogeographic patterns of genetic diversity in eastern Mediterranean water frogs were determined by geological processes and climate change in the Late Cenozoic. *Journal of Biogeography* **37:** 2111–2124.

Arthofer W, Schüler S, Steiner F, Schlick-Steiner BC. 2010. Chloroplast DNA-based studies in molecular ecology may be compromised by nuclear-encoded plastid sequence. *Molecular Ecology* **19:** 3853–3856.

Avise JC. 2000. *Phylogeography: the history and formation of species.* Cambridge: Harvard University Press.

Aydin Z, Ertekin AS, Långström E, Oxelman B. 2014. A new section of *Silene* (Caryophyllaceae) including a new species from South Anatolia, Turkey. *Phytotaxa* **178:** 098–112.

Bandelt HJ, Forster P, Röhl A. 1999. Median-joining networks for inferring intraspecific phylogenies. *Molecular Biology and Evolution* **16:** 37–48.

Barriel V. 1984. Phylogénie moléculaire et insertions-délétions de nucléotides. *Comptes Rendus de l'Académie des Sciences Paris* **317:** 693–701.

Bielejec F, Rambaut A, Suchard MA, Lemey P. 2011. SPREAD: spatial phylogenetic reconstruction of evolutionary dynamics. *Bioinformatics* **27:** 2910–2912.

Bittkau C, Comes HP. 2005. Evolutionary processes in a continental island system: molecular phylogeography of the Aegean *Nigella arvensis* alliance (Ranunculaceae) inferred from chloroplast DNA. *Molecular Ecology* **14:** 4065–4083.

Brosolo L, Mascle J, Loubrieu B. 2012. *Morphobathymetric map of the Mediterranean Sea*. Paris: CCGM/CGMW. UNESCO.

Cellinese N, Smith SA, Edwards EJ, Kim ST, Haberle RC, Avramakis M, Donoghue MJ 2009. Historical biogeography of the endemic Campanulaceae of Crete. *Journal of Biogeography* **36:** 1253–1269.

Comes HP, Kadereit JW. 1998. The effect of Quaternary climatic changes on plants distribution and evolution. *Trends in Plant Sciences* **3:** 432–438.

Condamine FL, Soldati L, Clamens AL, Rasplus JY, Kergoat GJ. 2013. Diversification patterns and processes of wingless endemic insects in the Mediterranean Basin: historical biogeography of the genus *Blaps* (Coleoptera: Tenebrionidae). *Journal of Biogeography* **40:** 1899–1913.

Coode MJE, Cullen J. 1967. *Silene* L. In: Davis PH, ed. *Flora of Turkey and the East Aegean Islands.* Edinburgh: Edinburgh University Press, 179–242.

Creutzburg N. 1958. *Probleme des Gebirgbaues und der Morphogenese auf Insel Kreta*. Freiburg: Freiburg Universität.

Davis PH. 1971. Distribution patterns in Anatolia with particular reference to Anatolia. In: Davis PH, Harper PC, Hedge JC, eds. *Plant life of South West Asia.* Edinburgh. Botanical Society of Edinburgh, 15–27.

Dermitzakis DM. 1990. Paleogeography, geodynamic processes and event stratigraphy during the late Cenozoic of the Aegean area. International Symposium on Biogeographical Aspects of Insularity. *Accademia Nazionale Lincei* **85:** 263–288.

Dermitzakis DM, Papanikolaou D. 1981. Palaeogeography and geodynamics of the Aegean region during the Neogene. *VIIth International Congress on Mediterranean Neogene* **4:** 245–289.

Dimopoulos P, Georgiadis T. 1992. Floristic and phytogeographical analysis of Mount Killini (NE Peloponnisos, Greece). *Phyton* **32:** 283–305.

Du Pasquier PE, Naciri Y, Jeanmonod D. 2015. Morphological analysis of the *Silene gigantea* complex (Caryophyllaceae) across the Balkan Peninsula, south-western Turkey and Cyprus. *Plant Systematics and Evolution* **301:** 2025–2042.

Đurović S, Schönswetter P, Marjan N, Tomović G, Frajman B. 2017. Disentangling relationships among the members of the *Silene saxifraga* alliance (Caryophyllaceae): phylogenetic structure is geographically rather taxonomically segregated. *Taxon* 66: in press.

Edh K, Widén B, Ceplitis A. 2007. Nuclear and chloroplast microsatellites reveal extreme population differentiation and limited gene flow in the Aegean endemic *Brassica cretica* (Brassicaceae). *Molecular Ecology* **16:** 4972–7983.

Excoffier L, Lischer HEL. 2010. Arlequin suite version 3.5: a new series of programs to perform population genetics analyses under Linux and Windows. *Molecular Ecology Resources* **10:** 564–567.

Frajman B, Oxelman B. 2007. Reticulate phylogenetics and phytogeographical structure of *Heliosperma* (Sileneae, Caryophyllaceae) inferred from chloroplast and nuclear DNA sequences. *Molecular Phylogenetics and Evolution* **43:** 140–155.

Frajman B, Eggens F, Oxelman B. 2009. Hybrid origins and homoploid reticulate evolution within *Heliosperma* (Sileneae, Caryophyllaceae) – a multigene phylogenetic approach with relative dating. *Systematic Biology* **58:** 328–345.

Fu YX. 1997. Statistical tests of neutrality of mutations against population growth, hitchhiking and background selection. *Genetics* **147:** 915–925.

Gantenbein B, Keightley PD. 2004. Rates of molecular evolution in nuclear genes of east Mediterranean scorpions. *Evolution* **58:** 2486–2497.

Ghazanfar SA. 1983. Cytological studies in the genus *Silene* L. *New Phytologist* **93:** 123–127.

Gielly J, Debussche M, Thompson JD. 2001. Geographic isolation and evolution of Mediterranean endemic *Cyclamen*: insights from chloroplast *trnL* (UAA) intron sequence variation. *Plant Systematics and Evolution* **230:** 75–88.

Goudet J. 1995. Fstat (version 1.2): a computer program to calculate F-statistics. *Journal of Heredity* **86:** 485–486.

Greenberg AK, Donoghue MJ. 2011. Molecular systematics and character evolution in Caryophyllaceae. *Taxon* **60:** 1637–1652.

Greuter W. 1970. Zur Paläogeographie une Florengeschiste der südlichen Ägäis. *Feddes Repertorium* **81:** 233–242.

Greuter W. 1995. Studies in Greek Caryophylloideae: *Agrostemma*, *Silene*, and *Vaccaria*. *Willdenowia* **25:** 105–142.

Greuter W. 1997. *Silene* L. In: Strid A, Tan K, eds. *Flora Hellenica*. Königstein: Koeltz Scientific Books, 239–323.

Guillot G. 2008. Inference of structure in subdivided populations at low levels of genetic differentiation the correlated allele frequencies model revisited. *Bioinformatics* **24:** 2222–2228.

Guillot G, Estoup A, Mortier F, Cosson JF. 2005a. A spatial statistical model for landscape genetics. *Genetics* **170:** 1261–1280.

Guillot G, Mortier F, Estoup A. 2005b. Geneland: a computer package for landscape genetics. *Molecular Ecology Notes* **5:** 712–715.

Hall TA. 1999. BioEdit: a user-friendly biological sequence alignment editor and analysis program for Windows 95/98/NT. *Nucleic Acids Symposium Series* **41:** 95–98.

Hamilton MB. 1999. Four primer pairs for the amplification of chloroplast intergenic regions with intraspecific variation. *Molecular Ecology* **8:** 521–523.

Hand R, Hadjikyriakou GN, Christodoulou CS, Frajman B. 2015. Multiple origins of dendroid shrubs in the eastern Mediterranean *Euphorbia hierosolymitana* group (Euphorbiaceae) with description of a new species, *Euphorbia*

lemesiana, from Cyprus. *Botanical Journal of the Linnean Society* **179**: 295-307.

Hand R, Hadjikyriakou GN, Christodoulou CS. eds. 2011. (continuously updated). Flora of Cyprus – a dynamic checklist. Last accessed 06.10.2016. Available at: http://www.flora-of-cyprus.eu/

Heled J, Drummond AJ. 2010. Bayesian inference of species trees from multilocus data. *Molecular Biology and Evolution* **27:** 570–580.

Ingvarsson PK, Ribstein S, Taylor DR. 2003. Molecular evolution of insertions and deletion in the chloroplast genome of *Silene*. *Molecular Biology and Evolution* **20:** 1737–1740.

Klopfstein S, Currat M, Excoffier L. 2006. The fate of mutations surfing on the wave of a range expansion. *Molecular Biology and Evolution* **23:** 482–490.

Kornilios P, Ilgas Ç, Kumlutaş Y, Lymberakis P, Moravec J, Sindaco R, Rastegar-Pouyani N, Afroosheh M, Giokas S, Fraguedakis-Tsolis S, Chondropoulos B. 2012. Neogene climatic oscillations shape the biogeography and evolutionary history of the Eurasian blindsnake. *Molecular Phylogenetics and Evolution* **62:** 856–873.

Krijgsman W, Stoica M, Vasiliev I, Popov VV. 2010. Rise and fall of the Paratethys Sea during the Messinian Salinity Crisis. *Earth Planetary Science Letters* **290:** 183–191.

Kryštufek B, Reed JM. 2004. Pattern and process in Balkan biodiversity. An overview. In: Griffiths HI, Kryštufek B, Reed JMM, eds. *Balkan biodiversity. Pattern and process in the European hotspot*. London: Kluwer Academic Publishers, 1–8.

Kürschner H, Raus T, Venter J. 1995. *Pflanzen der Türkei.* Wiesbaden: Quelle & Meyer Verlag.

Leuzinger M, Naciri Y, Du Pasquier PE, Jeanmonod D. 2015. Molecular diversity, phylogeography and relationships of the *Silene paradoxa* group of section *Siphonomorpha* (Caryophyllaceae). *Plant Systematics and Evolution* **301:** 265–278.

Lymberakis P, Poulakakis N, Manthalou G, Tsigenopoulos CS, Magoulas A, Mylonas M. 2007. Mitochondrial phylogeography of *Rana* (*Pelophylax*) populations in the eastern Mediterranean region. *Molecular Phylogenetics and Evolution* **44:** 115–125.

Manen JF, Barriera G, Loizeau PA, Naciri Y. 2010. The history of extant *Ilex* species (Aquifoliaceae): evidence of hybridization within a Miocene radiation. *Molecular Phylogenetics and Evolution* **57:** 961–977.

Meikle RD. 1977. *Flora of Cyprus.* Kew: The Bentham-Moxon Trust, Royal Botanic Gardens.

Möller M, Cronk QCB. 1997. Origin and relationships of *Saintpaulia* (Gesneriaceae) based on ribosomal DNA internal transcribed spacer (ITS) sequences. *American Journal of Botany* **87:** 956–965.

Montesinos D, García-Fayos P, Mateu I. 2006. Conflicting selective forces underlying seed dispersal in the endangered plant *Silene diclinis*. *International Journal of Plant Science* **167:** 103–110.

Naciri Y, Du Pasquier PE, Lundberg M, Jeanmonod D, Oxelman B. (in press). A phylogenetic circumscription of the *Silene* section *Siphonomorpha* (Caryophyllaceae) in the Mediterranean Basin. *Taxon*.

Naciri Y, Cavat F, Jeanmonod D. 2010. *Silene patula* (*Siphonomorpha*, Caryophyllaceae) in North Africa: a test of colonisation using chloroplast markers. *Molecular Phylogenetics and Evolution* **54:** 922–932.

Naciri Y, Linder P. 2015. Species identification and delimitation: the dance of the seven veils. *Taxon* **64:** 3–16.

Naciri Y, Manen JF. 2010. Potential DNA transfer from the chloroplast to the nucleus in *Eryngium alpinum* L. (Apiaceae). *Molecular Ecology Resources* **10:** 728–731.

Nei M. 1987. *Molecular evolutionary genetics.* New York: Columbia University Press.

Nei M, Chesser K. 1983. Estimation of fixation indices and gene diversities. *Annals of Human Genetics* **47:** 253–259.

Nielsen R, Wakeley J. 2001. Distinguishing migration from isolation: a Markov chain Monte Carlo approach. *Genetics* **158:** 885–896.

Nieto Feliner G. 2014. Patterns and processes in plant phylogeography in the Mediterranean Basin. A review. *Perspectives in Plant Ecology Evolution and Systematics* **16:** 265–278.

Parmakelis A, Stathi I, Chatzaki M, Simaiakis S, Spanos L, Louis C, Mylonas M. 2006a. Evolution of *Mesobuthus gibbosus* (Brullé, 1832) (Scorpiones: Buthidae) in the north-eastern Mediterranean region. *Molecular Ecology* **15:** 2883–2894.

Parmakelis A, Stathi I, Spanos L, Louis L, Mylonas M. 2006b. Phylogeography of *Lurus dufoureius* (Brullé, 1832) (Scorpiones, Luridae). *Journal of Biogeography* **33:** 251–260.

Percy DM, Argus GW, Cronk QC, Fazekas AJ, Kesanakurti PR, Burgess KS, Husband BC, Newmaster SG, Barrett SCH, Graham SW. 2014. Understanding the spectacular failure of DNA barcoding in willows (*Salix*): does this result from a trans-specific selective sweep? *Molecular Ecology* **23:** 4737–4756.

Perissoratis C, Conispoliatis N. 2003. The impact of sea-level changes during latest Pleistocene and Holocene times on the morphology of the Ionian and Aegean seas (SE Alpine Europe). *Marine Geology* **196:** 145–156.

Polunin O. 1980. *Flowers of Greece and the Balkans. A field guide.* Oxford: Oxford University Press.

Posada D, Crandall KA. 2001. Intraspecific gene genealogies: trees grafting into networks. *Trends in Ecology and Evolution* **16:** 37–45.

Poulakakis N, Kapli P, Lymberakis P, Trichas A, Vardinoyannis K, Sfenthourakis S, Mylonas M. 2015. A review of phylogeographic analyses of animals taxa from the Aegean and surrounding regions. *Journal of Zoological Systematics and Evolutionary Research* **53:** 18–32.

Poulakakis N, Lymberakis P, Tsigenopoulos CS, Magoulas A, Mylonas M. 2005. Phylogenetic relationship and evolutionary history of snake-eyed skink *Ablepharus kitaibelii* (Sauria: Scincidae). *Molecular Phylogenetics and Evolution* **34:** 245–256.

Poulakakis N, Paschalia K, Kardamaki A, Skourtanioti E, Göcmen B, Çetin I, Kumlutaş Y, Avcis A, Lymberakis P. 2013. Comparative phylogeography of six herpetofauna species in Cyprus: late Miocene to Pleistocene colonization routes. *Biological Journal of the Linnean Society* **108:** 619–635.

Rautenberg A, Hathaway L, Oxelman B, Prentice HC. 2010. Geographic and phylogenetic patterns in *Silene* section *Melandrium* (Caryophyllaceae) as inferred from chloroplast and nuclear DNA sequences. *Molecular Phylogenetics and Evolution* **57:** 978–991.

R Development Core Team. 2012. *R: a language and environment for statistical computing*. Vienna: R Foundation for Statistical Computing.

Rechinger KH. 1943. Flora Aegea. Flora der Inseln und Halbinsel des Ägäischen Meeres. *Denkschriften der Kaiserlichen Akademie der Wissenschaften* **105**: **1. Halbband**: 1-924.

Rechinger KH. 1950. Grundzüge der Pflanzenverbreitung in der Agaïs I-III. *Vegetatio* **2:** 55–119, 239–308, 365–386.

Rechinger KH, Rechinger-Moser F. 1951. Phytogeographia Aegaea. *Denkschriften der Kaiserlichen Akademie der Wissenschaften* **105**: **2. Halbband, 2. Abt**.: 1-208 .

Sevgili H, Çıplak B, Heller KG, Demirsoy A. 2006. Morphology, bioacoustic and phylogeography of the *Isophya major* group (Orthoptera: Tettigoniidae: Phaneropterinae): a species complex occurring in Anatolia and Cyprus. *European Journal of Entomology* **103:** 657–671.

Simaiakis SM, Dimopoulos P, Mitrakos A, Mylonas M, Parmakelis A. 2012. The evolutionary history of the Mediterranean centipede *Scolopendra cingulata* (Latreille, 1829) (Chilopoda: Scolopendridae) across the Aegean archipelago. *Biological Journal of the Linnean Society* **105:** 507–521.

Simmons MP, Ochoterena H. 2000. Gaps as characters in sequences-based phylogenetic analyses. *Systematic Biology* **49:** 369–381.

Sloan DB, Oxelman B, Rautenberg A, Taylor DR. 2009. Phylogenetic analysis of mitochondrial substitution rate variation in the angiosperm tribe Sileneae. *BMC Evolutionary Biology* **9:** 260.

Soltis DE, Kuzoff RK. 1995. Discordance between nuclear and chloroplast phylogenies in the *Heuchera* group (Saxifragaceae). *Evolution* **49:** 727–742.

Staats M, Cuenca A, Richardson JE, Vrielink-van Ginkel R, Petersen G, Seberg O, Bakker FT. 2011. DNA damage in plant herbarium tissue. *PLoS One* **6:** e28448.

Stephens M, Smith NJ, Donnelly P. 2001. A new statistical method for haplotype reconstruction from population data. *American Journal of Human Genetics* **68:** 978–989.

Stöck M, Sicilia A, Belfiore NM, Buckley D, Lo Brutto S, Lo Valvo M, Arculeo M. 2008. Post-Messinian evolutionary relationships across the Sicilian channel: mitochondrial and nuclear markers link a new green toad from Sicily to African relatives. *BMC Evolutionary Biology* **8:** 56.

Strid A. 1986. The mountain flora of Greece with special reference to the Anatolian element. *Proceedings of the Royal Society Edinburgh* **89b:** 59–68.

Strid A. 1996. Phytogeographia Aegea and the Flora Hellenica Database. *Annalen des Naturhistorischen Museums in Wien* **98B:** 279–289.

Strid A. 2016. Atlas of the Aegean Flora. Part 2: maps. *Englera* **33(2):** 1-878.

Strid A, Andersson IA. 1985. Chromosome numbers of Greek mountain plants. An annotated list of 115 species. *Botanische Jahrbücher für Systematik, Pflanzengeschichte und Pflanzengeographie* **107:** 203–228.

Strid A, Tan K. 1997. *Flora Hellenica*. Königstein: Koeltz Scientific Books.

Suc JP, Clauzon G. 1996. La crise de salinité messinienne, une histoire fabuleuse. *Bulletin de la Société Botanique de Fribourg Sciences Naturelles* **85:** 9–23.

Tajima F. 1983. Evolutionary relationship of DNA sequences in finite populations. *Genetics* **105:** 437–460.

Taylor DR, Keller SR. 2007. Historical range expansion determines the phylogenetic diversity introduced during contemporary species invasion. *Evolution* **61:** 334–345.

Thompson JD. 2005. *Plant evolution in the Mediterranean*. New York: Oxford University Press

Triantis KA, Mylonas M. 2009. Greek islands, biology. In: Gillespie RG, Clague DA, eds. *Encyclopedia of islands*. Oakland: University of California Press, 388–392.

Trigas P, Iatrou G, Karetsos G. 2007. Species diversity, endemism and conservation of the family Caryophyllaceae in Greece. *Biodiversity and Conservation* **16:** 357–376.

Trigas P, Tsiftsis S, Tsiripidis I, Iatrou G. 2012. Distribution patterns and conservation perspectives of the endemic flora of Peloponnese (Greece). *Folia Geobotanica* **47:** 421–439.

Troia A, Raimondo FM, Geraci A. 2012. Does genetic population structure of *Ambrosina basii* L. (Araceae, Ambrosineae) attest a post-Messinian land-bridge between Sicily and Africa? *Flora* **207:** 646–653.

Tzedakis PC. 2004. The Balkans as prime glacial refugial territory of European temperate trees. In: Griffiths HI, Kryštufek B, Reed JMM, eds. *Balkan biodiversity. Pattern and process in the European hotspot*. London: Kluwer Academic Publishers, 49–68.

Wolfe KH, Sharp PM. 1988. Identification of functional open reading frames in chloroplast genomes. *Gene* **66:** 215–222.

Yıldız K. 2006. Morphological and palynological investigation on *Silene gigantea* L. var. *gigantea* and *Silene behen* L. (Caryophyllaceae) distributed in western Anatolia and northern Cyprus. *Turkish Journal of Botany* **30:** 105–119.

Yıldız K, Çırpıcı AH. 2013. Taxonomic revision of *Silene* (Caryophyllaceae) sections *Siphonomorpha, Lasiostemones, Sclerocalycinae, Chloranthae, Tataricae* and *Otites* in Turkey. *Turkish Journal of Botany* **37:** 191–218.

Yıldız K, Mınarecı E, Çırpıcı A. 2009. Karyotypic study on *Silene*, section *Lasiostemones* species from Turkey. *Caryologia* **62:** 134–141.

Yıldız K, Mınarecı E, Çırpıcı A, Dadandi MY. 2008. A karyotypic study on *Silene*, section *Siphonomorpha* species of Turkey. *Nordic Journal of Botany* **26:** 368–374.

Zohary M. 1973. *Geobotanical foundations of the Middle East*. Stuttgart: Gustav Fischer Verlag.

SUPPORTING INFORMATION

Additional Supporting Information may be found in the online version of this article at the publisher's website:

Appendix 1. A Rechinger's phytogeographic divisions of Greece (dotted lines) and divisions adopted in the *Flora Hellenica* (broken lines) and drawn after Strid (1996). **B** Phytogeographic divisions in Turkey, drawn after Kürschner Raus & Venter (1995).

Appendix 2. PCRs were performed in a total volume of 20 µL with 2 µL 10× reaction buffer (100 mM Tris-HCL), 2 µL $MgCl_2$ (25 mM), 0.4 µL dNTP (10 mM each, Promega), 0.2 µL 5% bovine albumin serum (BSA, 0.4 µL for herbarium specimens), 1 µL each primer (100 µM, MWG-Biotech), 0.15 µL Taq polymerase (5U/µL, AmpliTaq®) and 12.25 µL purified water. PCR reaction included a step of denaturation of 6 min at 95°C, followed by 35 cycles with 1 min denaturation at 95°C, 30 s of annealing at 52°C, 45 s of extension at 72°C and a final extension of 7 min at 72°C. The pause was fixed at 10°C. For nested-PCR, the number of steps of the first PCR was reduced to 25. The PCR products were purified on plates (NucleoFast©, Macherey-Nagel) with an intermediate washing of 100 µL with purified water during 10 min. The purified DNA was resuspended in 50 µL pure water. For the Beckman sequencer, both plastid strands were sequenced separately in a 10 µL reaction mix with 1 µL purified PCR product, 4 µL purified water, 4 µL DTCS and 1 µL primers (0.5 mM). For the nuclear strands, the mix volume was reduced to 5 µL with 0.5 µL purified PCR product, 2 µL purified water, 2 µL DTCS and 0.5 µL primers (0.5 mM). For the ABI sequencer, plastid and nuclear strands were sequenced separately in a 5 µL reaction mix with 0.5 µL purified PCR product, 2 µL purified water, 0.5 µL TERM Big Dye, 1 µL 5× buffer solution and 1 µL primer (1 µM). Sequence reactions for the BigDye™ Sequencing kits (Applied Biosystems) included 25 cycles of 10 s denaturation at 96°C, 5 s annealing at 50°C and 4 min extension at 60°C. Sequence reactions for the GenomeLab™ Quick Start Kit (Beckman Coulter) included 30 cycles of 20 s denaturation at 96°C, 20 s annealing at 50°C and 4 min extension at 60°C.

Appendix 3. List of the studied individuals of *Silene gigantea* with their voucher numbers, haplotype names and GenBank accession numbers.

Appendix 4. Number of specimens sequenced for each marker (*trnH-psbA, trnS-trnG* and ITS) and their combination on a total of 285 individuals, and DNA amplification success rates depending on material origin, fresh (222 individuals) or herbarium (61 individuals) of the *Silene gigantea* complex.

Appendix 5. Median joining network using the nuclear marker ITS on 189 individuals. The size of each circle is proportional to the corresponding ribotype frequency in the species. The black node corresponds to a missing or unsampled ribotype. Mutational steps are indicated in red. *Silene gigantea* subsp. *gigantea* is in red, *S. gigantea* subsp. *hellenica* in green, *S. gigantea* subsp. *rhodopea* in blue and the Epirus group in yellow.